The role of an unusual cyclin in control of cell cycle entry and cell size in budding yeast

Amanda Brambila, Joao A. Paulo*, Steven Gygi* and Douglas R. Kellogg

Department of Molecular, Cell and Developmental Biology
University of California, Santa Cruz
*Department of Cell Biology, Harvard Medical School

Abstract

Entry into the cell cycle in late G1 phase occurs only when sufficient growth has occurred. In budding yeast, a cyclin called Cln3 is thought to link cell cycle entry to cell growth. Cln3 accumulates during growth in early G1 phase and eventually triggers accumulation of late G1 cyclins that drive cell cycle entry. All current models assume that Cln3 works solely in G1 phase and activates Cdk1 to initiate accumulation of late G1 cyclins solely via transcriptional mechanisms. Here, we show that Cln3 can influence accumulation of late G1 cyclin proteins via post-transcriptional mechanisms. Furthermore, proteomic analysis of the effects of loss- or gain-of-function of Cln3 found no clear evidence that Cln3 activates Cdk1, and an analysis of Cln3 binding to Cdk1 failed to find clear evidence that Cln3 can bind directly to Cdk1, which suggests that Cln3 could carry out functions independently of Cdk1, similar to mammalian cyclin F. Finally, we show that Cln3 has functions in mitosis that strongly influence cell size. Together, these discoveries reveal surprising new functions for Cln3 that challenge current models for control of cell cycle entry and cell size.

Introduction

The decision to enter a new round of cell division is amongst the most consequential decisions in the life of a cell. Entry into the cell cycle occurs only when sufficient growth has occurred and only when there are sufficient nutrients for further growth. In animal cells, cell cycle entry is also controlled by growth factors, which ensure that cell division occurs at an appropriate time and place. Defects in signals that control cell cycle entry are a primary cause of cancer.

The mechanisms that initiate cell cycle entry are poorly understood. In budding yeast, decades of work led to a canonical model in which a cyclin called Cln3 appears in early G1 phase and activates Cdk1 (Carter and Sudbery, 1980; Cross, 1988, 1989; Nash *et al.*, 1988; Hadwiger *et al.*, 1989; Richardson *et al.*, 1989; Tyers *et al.*, 1992, 1993). The Cln3/Cdk1 complex then directly phosphorylates and inactivates Whi5, a transcriptional repressor that binds and inhibits two transcription factors, referred to as SBF and MBF, that drive transcription of late G1 cyclins, as well as hundreds of additional genes (Costanzo *et al.*, 2004; de Bruin *et al.*, 2004; Iyer *et al.*, 2001; Koch *et al.*, 1996; Nasmyth and Dirick, 1991; Ferrezuelo *et al.*, 2010; Tyers *et al.*, 1993; Wijnen *et al.*, 2002; Jorgensen *et al.*, 2002; Spellman *et al.*, 1998; Bean *et al.*, 2005). Thus, Cln3-dependent inactivation of Whi5 has been thought to initiate transcription of late G1 cyclins, which is the critical molecular event that marks cell cycle entry. Genetic analysis suggests that Cln3 and Whi5 link cell cycle entry to cell growth. For example, loss of *WHI5* causes premature cell cycle entry before sufficient growth has occurred, leading to a reduced cell size (Jorgensen *et al.*, 2002; Costanzo *et al.*, 2004; de Bruin *et al.*, 2004). Similarly, loss of Cln3 causes delayed cell cycle entry and increased cell size, while overexpression of Cln3 leads to premature cell cycle entry and reduced cell size (Sudbery *et al.*, 1980; Cross, 1988, 1989; Nash *et al.*, 1988; Tyers *et al.*, 1993; Jorgensen and Tyers, 2004).

The canonical model has provided an important framework for analysis of cell cycle entry and has strongly influenced models for how cell growth influences cell cycle entry. However, a number of observations cannot be explained by the model. For example, over-expression of Cln3 causes a large reduction in the size of *whi5*Δ cells, which indicates that Cln3 has critical targets other than Whi5 (Costanzo *et al.*, 2004; Wang *et al.*, 2009). Furthermore, two independent studies failed to detect Cln3-dependent phosphorylation of Whi5 in vivo (Bhaduri *et al.*, 2015; Kõivomägi *et al.*, 2021), and there are conflicting reports regarding whether Cln3 is associated with active Cdk1 (Tyers *et al.*, 1992, 1993; Nasmyth, 1993; Costanzo *et al.*, 2004; Schneider *et al.*, 2004; Kõivomägi *et al.*, 2021). Canonical cyclins bind Cdk1 with very high affinity to form a tight stoichiometric complex. However, no studies have shown that it is possible to purify a stoichiometric complex containing Cln3 and Cdk1, and no studies have shown that purified Cln3 can activate purified Cdk1. The extent to which Cln3 can bind and activate Cdk1 therefore remains unclear and it is possible that Cln3 carries out kinase-independent functions, similar to mammalian cyclin F (D'Angiolella *et al.*, 2013).

A further concern is that it has been assumed that Cln3 exerts all its key functions in G1 phase, especially with respect to control of cell size. However, there are two peaks of Cln3 protein during the cell cycle – one in G1 phase and a second in mitosis (Landry *et al.*, 2012; Zapata *et al.*, 2014; Litsios *et al.*, 2019). The functions of Cln3 during mitosis are unknown. Since most growth of a yeast cell occurs during bud growth in mitosis (Leitao and Kellogg, 2017), it is possible that mitotic functions of Cln3 play a major role in Cln3's ability to influence cell size.

Here, we tested key aspects of the canonical model for cell cycle entry in yeast, while also searching for Whi5-independent functions of Cln3. The results suggest that models for the functions of Cln3 and Whi5 needs to be re-evaluated.

Results

Cln3 can influence production of Cln2 protein via Whi5-independent mechanisms

We first investigated the mechanism by which overexpression of Cln3 makes *whi5*Δ cells smaller. Since Cln3 is expressed in mitosis, it is possible that mitotic functions of Cln3 drive a reduction in cell size in *whi5*Δ cells (Landry *et al.*, 2012; Zapata *et al.*, 2014). It is also possible that Cln3 works in G1 phase to promote production of late G1 cyclins via mechanisms that are independent of Whi5. To investigate further, we first determined whether loss- or gain-of-function of Cln3 influences production of Cln2 protein in *whi5*Δ cells. We used *cln3*Δ to test loss of Cln3 function. To achieve gain-of-function of Cln3, we utilized the *cln3-Δ177* allele, which lacks C-terminal PEST sequences that targets it for rapid turnover via ubiquitin-dependent proteolysis (Nash *et al.*, 1988). Previous work found that *cln3-Δ177* results in a 10-fold increase in Cln3 protein levels, as well as a large decrease in cell size (Sudbery *et al.*, 1980; Tyers *et al.*, 1992). A 3XHA-tagged version of Cln2 was used to assay levels of Cln2 protein. We synchronized wild type, *whi5*Δ*, whi5*Δ *cln3-Δ177* and *whi5*Δ *cln3*Δ cells in G1 phase using mating pheromone and assayed production of *Cln2-3XHA* during the cell cycle at 10 minute intervals (**Figure 1A,B**).

A previous study found that loss of *WHI5* accelerates production of Cln2 mRNA (Costanzo *et al.*, 2004). Here, we found that loss of *WHI5* accelerated production of Cln2 protein by approximately 10 minutes relative to wild type. Furthermore, overexpression of Cln3 accelerated production of Cln2 protein in *whi5*Δ cells, while *cln3*Δ delayed production of Cln2.

A concern with the use of *cln3*Δ and *cln3-Δ177* is that they cause substantial cell size defects that could indirectly influence the timing of cell cycle entry. Therefore, as a further means of testing the effects of Cln3 overexpression, we utilized cells that express an extra copy of wild type *CLN3* from the inducible *GAL1* promoter, which allowed us to test the immediate effects of increased Cln3 levels in otherwise normal cells. Wild type and *GAL1-CLN3* cells were arrested in G1 phase in media containing 2% glycerol and 2% ethanol to repress transcription of *GAL1-CLN3*. Expression of *GAL1-CLN3* was induced with 2% galactose 30 minutes before release from the G1 arrest. We again found that overexpression of Cln3 accelerated production of Cln2 in *whi5*Δ cells (**Figure 1C,D**). The effects of full length *CLN3* expressed from the *GAL1* promoter appeared to be stronger than the effects of *cln3-Δ177*, as *GAL1-CLN3* caused a larger increase in the amount of Cln2 protein (compare **Figures 1B and 1D**).

Cln2 protein expression remained strongly periodic in both *whi5*Δ and *whi5*Δ *cln3*Δ cells (**Figure 1A**). A previous study found that expression of *CLN2* mRNA remains strongly periodic in *whi5*Δ cells (Costanzo *et al.*, 2004). If Whi5 was the primary mechanism that prevents expression of late G1 cyclins in early G1 phase one would expect to see a general de-repression of Cln2 expression throughout G1 phase. These observations therefore indicate that Whi5-independent mechanisms play a major role in prevention of Cln2 protein expression in early G1 phase, and that there are important mechanisms that enforce periodic expression of Cln2 that operate independently of Whi5 and Cln3.

Cln3 can influence levels of Cln2 protein via post-transcriptional mechanisms

Cln3 could control transcription of Cln2 via mechanisms that are independent of Whi5, but dependent upon other features of the Cln2 promoter. For example, Cln3 could directly activate SBF or other components of the transcriptional machinery at Cln2 promoters. Alternatively, Cln3 could also influence production of Cln2 protein via post-transcriptional mechanisms. To distinguish these possibilities, we created a strain in which transcription of *3XHA-CLN2* is

controlled by the *MET25* promoter (*MET25-3XHA-CLN2*), thereby eliminating normal control of Cln2 transcription. The *MET25* promoter drives a low basal level of transcription when methionine is present in the growth medium. Removal of the methionine leads to an approximately 10-fold increase in transcription. Previous studies have shown that overexpression of Cln3 does not influence transcription of *MET25*, and that SBF and MBF cannot be detected at the *MET25* promoter (Iyer *et al.*, 2001; Ferrezuelo *et al.*, 2010). Here, we utilized the low uninduced basal transcription from the *MET25* promoter to express *3XHA-CLN2*. We found that *cln3-Δ177* advanced expression of Cln2 protein in *MET25-3XHA-CLN2* cells (**Figures 2A,B**). Conversely, *cln3Δ* caused delayed and reduced expression of Cln2 protein. These results show that Cln3 can influence expression of Cln2 protein via mechanisms that work independently of the normal transcriptional control of the *CLN2* gene. We obtained the same result using an independently constructed set of strains in which *GAL1-CLN3* was used to overexpress *CLN3* (**Figure 3**), and in strains where Cln2 was tagged with a C-terminal 9Myc tag (not shown).

Cln2 protein expressed from the *MET25* promoter showed cell cycle periodicity, which provides further evidence that post-transcriptional mechanisms play a significant role in the mechanisms that drive periodic expression of Cln2 protein (**Figure 2A,B**). Previous studies have shown that constitutive expression of *CLN1* from the very strong *GAL1* promoter can rescue the inviability of *cln1Δ cln2Δ cln3Δ* cells (Richardson *et al.*, 1989). Although *GAL1-CLN1 cln2Δ cln3Δ* cells have an abnormal morphology, this observation shows that regulation of transcription is not required for the essential functions of late G1 cyclins, and it suggests that post-transcriptional mechanisms likely play an important role in regulating late G1 cyclins.

Cln3 requires Swi6 to influence Cln2 protein levels

Cln3 is thought to influence transcription of late G1 cyclins via two transcription factors, known as SBF and MBF. SBF is a dimer composed of Swi6 and a DNA binding subunit called Swi4 (Andrews and Herskowitz, 1989; Andrews and Moore, 1992). Similarly, MBF is a dimer of Swi6 and a DNA binding subunit called Mbp1 (Siegmund and Nasmyth, 1996). Loss of Swi4 or Swi6 reduces, but does not eliminate, transcription of *CLN2* and causes delayed cell cycle entry and a large increase in cell size (Nasmyth and Dirick, 1991; Wijnen *et al.*, 2002). Key phenotypic effects of *CLN3* over-expression are dependent upon Swi6. For example, overexpression of *CLN3* does not cause reduced cell size in *swi6Δ* cells and fails to drive premature cell cycle entry or premature transcription of *CLN1* (Nasmyth and Dirick, 1991; Wijnen *et al.*, 2002). Cln3 co-immunoprecipitates with Swi6 and has been detected at SBF promoters in chromatin IP experiments, which suggests that Cln3 could directly influence transcription via Swi6 (Wang *et al.*, 2009; Kõivomägi *et al.*, 2021).

No previous studies have investigated the effects of Cln3 on production of late G1 cyclin proteins in *swi6Δ* cells. Here, we tested whether loss of *SWI6* influences accumulation of Cln2 in *MET25-3XHA-CLN2* cells. In the presence of *SWI6*, *GAL1-CLN3* advanced expression of Cln2 protein, as expected (**Figure 3**). *GAL1-CLN3* also advanced expression of the mitotic cyclin Clb2, which indicated that subsequent cell cycle steps were also advanced. Loss of Swi6 caused a loss of periodic expression of Cln2 protein in the *MET25-3XHA-CLN2* cells. Furthermore, overexpression of *CLN3* had no effect on expression of Cln2 protein in *MET25-3XHA-CLN2 swi6Δ* cells. Together, these observations suggest that Swi6 influences post-transcriptional mechanisms that are required for periodic expression of Cln2 protein. The data further suggest that Cln3 modulates levels of Cln2 protein at least partly via Swi6-dependent mechanisms that act after transcription of the *CLN2* gene. However, we note that *swi6Δ* cells are barely viable and rapidly

accumulate suppressor mutations. Furthermore, Swi6 controls the transcription of hundreds of genes, which means that loss of *SWI6* will have highly pleiotropic effects. Together, these considerations make it difficult to interpret the effects of *swi6*Δ. Transcription of *CLN2* appeared to be repressed in early G1 phase in all four *MET25-3XHA-CLN2* strains, which suggests the possibility that post-transcriptional mechanisms repress accumulation of Cln2 protein in early G1 phase. Potential models to explain these observations are considered in the Discussion.

Cln3 can influence cell size via mechanisms that are independent of transcriptional control of Cln1 and Cln2

Cln3 has been thought to influence cell size by regulating transcription of the late G1 cyclins (Cross, 1990; Tyers *et al.*, 1993; Wijnen *et al.*, 2002; Ferrezuelo *et al.*, 2010). To further investigate, we tested whether overexpression of *CLN3* influences cell size in a strain in which normal transcriptional control of both *CLN1* and *CLN2* has been eliminated. To do this, we created a strain in which the *CLN1* gene was deleted and *CLN2* was controlled by the *MET25* promoter (*MET25-3XHA-CLN2 cln1*Δ). We then integrated a copy of the wild type *CLN3* gene under the control of the *GAL1* promoter. When grown in dextrose to repress expression of *GAL1-CLN3*, the *MET25-3XHA-CLN2 cln1*Δ *GAL1-CLN3* cells were larger than wild type (**Figure 4A**). When grown in 2% galactose, overexpression of *CLN3* drove a large decrease in the size of *MET25-3XHA-CLN2 cln1*Δ cells (**Figure 4B**). The fact that Cln3 can drive a decrease in cell size in *MET25-3XHA-CLN2 cln1*Δ cells provides further evidence that Cln3 can influence cell size via mechanisms that are independent of transcriptional control of *CLN1* and *CLN2*.

Cln3 carries out functions in mitosis that influence cell size

Cln3 has been thought to exert all its effects in G1 phase. However, there is a second peak of Cln3 protein in mitosis (Landry *et al.*, 2012; Zapata *et al.*, 2014; Litsios *et al.*, 2019). Since most growth of budding yeast cells occurs during mitosis (Leitao and Kellogg, 2017), a mitotic function of Cln3 could make a major contribution to the effects of Cln3 on cell size. To investigate further, we used microscopy to analyze how loss- or gain-of-function of Cln3 influences the duration and extent of bud growth in mitosis. Since effects of Cln3 on cell size in G1 phase could influence growth in mitosis, we used conditional alleles to inactivate or overexpress Cln3 after cells passed through G1 phase. Conditional overexpression of Cln3 was achieved by expression of *CLN3* from the inducible *GAL1* promoter. Conditional inactivation of Cln3 was achieved with an auxin inducible degron version of *CLN3* (*cln3-AID*) (Nishimura *et al.*, 2009). The *cln3-AID* allele caused a modest increase in cell size in the absence of auxin, which indicated that the AID tag caused decreased function of Cln3. Prolonged growth of *cln3-AID* cells in the presence of auxin caused a larger increase in cell size, although the increase was not as large as the increase caused by *cln3*Δ, which indicated that the *cln3-AID* allele caused a partial loss of function of Cln3 (**Figure 5 – Figure Supplement 5**).

GAL1-CLN3 cells were arrested in G1 phase in media containing 2% glycerol and 2% ethanol to repress the *GAL1* promoter. Cells were released from the arrest and galactose was added to induce expression of *CLN3* when 15% cells had undergone bud emergence. To analyze loss of function, *cln3-AID* cells were released from a G1 arrest and auxin was added when 40-50% of the cells had undergone bud emergence. We induced gain- or loss-of-function of *CLN3* at different times relative to bud emergence because auxin-induced destruction of AID-tagged proteins occurs relatively rapidly (10-15 minutes), whereas high-level expression of proteins from the *GAL1* promoter occurs somewhat more slowly (20-30 minutes).

The durations of metaphase and anaphase were analyzed in single cells using a fluorescently tagged spindle pole protein, as previously described (Leitao and Kellogg, 2017; Jasani *et al.*, 2020). The spindle poles in wild type control cells were tagged with mCherry, while the spindle poles in *cln3-AID* and *GAL1-CLN3* were tagged with GFP, which allowed analysis of control and experimental cells simultaneously under identical conditions. Cell growth was analyzed by measuring the size of the daughter bud as a function of time.

Overexpression of Cln3 caused a decrease in the durations of both metaphase and anaphase, as well as a decrease in the size at which daughter buds complete metaphase and anaphase (**Figures 5A,B**). Conversely, loss of function of Cln3 caused an increase in the duration of metaphase and an increase in daughter bud size at the end of metaphase (**Figures 5C,D**). Loss of function of Cln3 did not cause a statistically significant change in the duration of anaphase. Together, these data show that Cln3 can influence the duration and extent of growth in mitosis.

An unbiased search for targets of Cln3-dependent regulation

The preceding experiments show that Cln3 can influence expression of Cln2 protein via mechanisms that are independent of Whi5 or any other proteins that act at the *CLN2* promoter. Furthermore, the data suggest that Cln3 has important targets during bud growth in mitosis that influence cell size. Thus, key targets of Cln3 function remain to be discovered. To search for these targets, we used proteome-wide mass spectrometry to identify proteins that show changes in phosphorylation in response to loss- or gain-of-function of *CLN3*. Wild type, ***cln3*Δ** and ***cln3-Δ177*** cells were grown to log phase and quantitative mass spectrometry was used to compare protein phosphorylation across the proteome. We used asynchronous cells because we wanted to detect changes in both G1 phase targets and mitotic targets of Cln3. A concern was that some changes in phosphorylation might only occur during specific cell cycle changes, which could be missed in an asynchronous population. However, the *cln3-Δ177* protein lacks C-terminal sequences that target it for destruction, which means that it is expressed throughout the cell cycle and at 10-fold higher levels than wild type Cln3 protein. One would therefore expect to detect hyperphosphorylation of targets of Cln3-Cdk1 in *cln3-Δ177* cells.

Since Cln3 is thought to activate Cdk1, we first examined the data for changes in phosphorylation. Changes in phosphorylation were calculated as a log2 transformation of the ratio of phosphorylated peptide in mutant cells over unphosphorylated peptide in wild type cells. Thus, a negative log2 ratio corresponds to a loss of phosphorylation in a mutant background, whereas a positive log2 ratio corresponds to a gain of phosphorylation. We used a log2 ratio of +/-1, corresponding to a 2-fold change in phosphorylation, as an arbitrary cutoff for identification of substantial changes in phosphorylation. The full data set is shown in **Supplemental Table 1**.

Proteins that are targets of Cln3/Cdk1 activity should show decreased phosphorylation at minimal Cdk1 consensus sites (S/TP) in ***cln3*Δ** cells and increased phosphorylation in ***cln3-Δ177*** cells. **Table 1** shows peptides that underwent a substantial loss of phosphorylation in ***cln3*Δ** cells, while **Table 2** shows peptides that underwent a gain of phosphorylation in ***cln3-Δ177*** cells. The data show little evidence of Cdk1-dependent phosphorylation. For example, there was no correspondence between the proteins that showed a substantial loss of phosphorylation in ***cln3*Δ** cells and the proteins that showed a substantial gain of phosphorylation in ***cln3-Δ177*** cells (**compare Tables 1 and 2**). To investigate further, we searched the data for sites that correspond to the minimal Cdk1 consensus sequence (S/TP) and show a loss of phosphorylation in ***cln3*Δ** and a gain of phosphorylation in ***cln3-Δ177***. Of the 54 peptides that showed a greater than two-fold loss of phosphorylation in ***cln3*Δ** cells, only 10 included a minimal Cdk1 consensus site. Of

these, only 5 showed a gain of phosphorylation in *cln3-Δ177* cells (highlighted in green in **Table 1**), and in each case the gain was below the threshold log2 ratio of -1 (log2 ratios of 0.499 to 0.667). Similarly, of the 82 peptides that showed a substantial gain of phosphorylation in *cln3-Δ177* cells, only 16 included a minimal Cdk1 consensus site. Of these, only 7 showed loss of phosphorylation in *cln3Δ* cells (highlighted in green in **Table 2**), and again in each case the loss of phosphorylation was below the threshold log2 ratio of +/-1 (log2 ratios of -0.040 to -0.947). Furthermore, the magnitude of the changes in phosphorylation indicated by the log2 ratios were lower than one might expect for a protein kinase. No peptides showed changes in log2 ratios greater than +/-2. For comparison, we found that loss of function of the Elm1 kinase in budding yeast causes 90 peptides to undergo changes in log2 ratios of greater than +/-2.

Whi5 was not identified by the mas-spec analysis, consistent with previous studies that found no evidence for Cln3-dependent phosphorylation of Whi5 (Bhaduri *et al.*, 2015; Kõivomägi *et al.*, 2021). A previous study that utilized a Cln3-Cdk1 fusion protein suggested that Cln3 activates Cdk1 to phosphorylate the C-terminal domain of RNA polymerase II, which contains multiple repeats of a sequence that includes minimal Cdk1 consensus sites. The C-terminal repeats of RNA polymerase II do not contain sites for the proteases used to generate peptides for mass spectrometry and would therefore not be detected in this analysis.

Overall, the analysis identified no minimal Cdk1 consensus sites that showed both a substantial increase in phosphorylation in *cln3-Δ177* cells and a substantial loss of phosphorylation *cln3Δ* cells. Furthermore, the peptides that showed loss of phosphorylation at a minimal Cdk1 consensus site in *cln3Δ* cells and a gain of phosphorylation in *cln3-Δ177* cells (highlighted in green in **Tables 1 and 2)** identified only 11 proteins: Rox1, Fin1, Tos4, YDR348C, Rpl12b, Ash1, Snf2, Nop10, Dsl1, and Caf120. None of these have been shown to play roles in the control of cell cycle entry or cell size. Two transcription factors called Ace2 and Ash1 that bind the Cln3 promoter were identified in *cln3-Δ177* cells (**Table 2**). In each case, *cln3-Δ177* caused a substantial increase in phosphorylation at a single site that corresponds to a minimal Cdk1 consensus site. On Ace2, the same site also showed a small increase in phosphorylation on *cln3Δ* cells, whereas on Ash1 the same site showed a likely negligible decrease in *cln3Δ* cells. The apparent increase in phosphorylation of these factors in *cln3-Δ177* cells could suggest that transcription of *CLN3* is controlled by Cln3-dependent positive feedback. However, a previous study found that exchanging the *CLN3* promoter for a heterologous constitutive promoter had no effect on cell size control, which suggests that transcriptional control of *CLN3* does not play a major role in control of cell size (Di Talia *et al.*, 2009).

Cln3 does not show typical binding to Cdk1

The phosphoproteomic data did not provide clear clues to how Cln3 influences Cln2 levels, or how Cln3 influences the duration and extent of growth in mitosis. However, the phosphoproteomic approach is predicated on the idea that Cln3 executes its functions via binding and activation of Cdk1. All of the other major cyclins in budding yeast bind Cdk1 to form a tight stoichiometric complex that can be purified under high salt conditions (Kõivomägi *et al.*, 2011). However, there are conflicting reports regarding whether Cln3 can bind and activate Cdk1. One recent study found that it was not possible to purify a Cln3/Cdk1 complex and resorted to using a Cln3-Cdk1 fusion protein to test whether Cln3 can activate Cdk1 (Kõivomägi *et al.*, 2021). Another well-controlled study found no kinase activity associated with Cln3 (Schneider *et al.*, 2004), while other studies detected weak kinase activity in Cln3 immunoprecipitates (Tyers *et al.*, 1992, 1993; Schneider *et al.*, 2004; Miller *et al.*, 2005). Several studies found that Cdk1 co-precipitates with

Cln3 but did not test for Cdk1-dependent kinase activity (Willems *et al.*, 1996; Bhaduri *et al.*, 2015). Importantly, there are no direct rigorous biochemical data showing that purified Cln3 can bind and activate purified Cdk1. Thus, the data suggest that Cln3 does not show typical binding and activation of Cdk1.

To investigate further, we immunoprecipitated Cln3 and Clb2 and tested for co-precipitation of Cdk1. Since Cln3 is a very low abundance protein, we expressed Cln3-3XHA from the strong *GAL1* promoter, while Clb2-3XHA was expressed from its own promoter. We did not detect any Cdk1 associated with Cln3, whereas Cdk1 robustly co-precipitated with Clb2 (**Figure 6A**).

We also used a previously published GST pull-down assay to test whether Cdk1 associates with Cln3 (Bhaduri *et al.*, 2015). In this approach, GST-cyclin fusion proteins expressed from the *GAL1* promoter are pulled out of crude extracts with glutathione beads and western blotting is used to test for associated Cdk1. We used this approach to compare the amount of Cdk1 associated with Clb2 and *cln3-10A*. The *cln3-10A* allele produces a stabilized version of Cln3 because it lacks C-terminal phosphorylation sites that target Cln3 for destruction. We detected a small amount of Cdk1 associated with GST-Cln3-10A, consistent with a previous study (**Figure 6B** (Bhaduri *et al.*, 2015)). However, the amount of Cdk1 associated with Cln3 was 6-fold lower than the amount of Cdk1 associated with GST-Clb2 in the same assay. We obtained a similar result when we compared the amount of Cdk1 that binds to GST-Cln3 and GST-Cln2 (not shown).

One explanation for the apparent weak interaction between Cln3 and Cdk1 could be that Cln3 binds Cdk1 indirectly. Previous studies have shown that Cln3 associates with components of the SCF^{Grr1} ubiquitin ligase complex, which targets G1 cyclins for proteolytic destruction (Willems *et al.*, 1996; Landry *et al.*, 2012). Components of SCF^{Grr1} also associate with Cln1 and Cln2 (Willems *et al.*, 1996; Skowyra *et al.*, 1997; Kishi and Yamao, 1998; Berset *et al.*, 2002; Landry *et al.*, 2012). We therefore considered the possibility that Cln3 associates with Cln2/Cdk1 via a complex that includes SCF^{Grr1}. We found that Cln2 can be detected in GST-Cln3-10A pulldowns, consistent with the possibility that Cdk1 detected in Cln3 pull-downs is due to an indirect association with Cln2-Cdk1 (**Figure 6C**). A previous study found that inactivation of Cdc34, an essential component of the SCF complex, leads to a 10-20 fold increase in the amount of kinase activity associated with Cln3 (Tyers *et al.*, 1992). Since inactivation of Cdc34 blocks ubiquitination of Cln2 and causes a large increase in the amount of Cln2, a potential explanation for this observation is that inactivation of Cdc34 leads to increased formation of a Cln3-SCF-Cln2/Cdk1 complex in which the increased kinase activity associated with Cln3 is due to Cln2/Cdk1.

Our results, combined with previously published data, show that Cln3 does not show typical binding to Cdk1. Moreover, the data thus far can not rule out the possibility that Cln3 binds Cdk1 indirectly. A definitive answer to the question of whether Cln3 can bind and activate Cdk1 will require reconstitution experiments using purified Cln3 and Cdk1. Importantly, the unusual behavior of Cln3 suggests that a substantial fraction of Cln3 may not be directly associated with Cdk1 in vivo, and the data therefore do not rule out the possibility that Cln3 carries out functions independently of Cdk1, in the same way that the mammalian cyclins E and F are thought to carry out functions independently of Cdk activity (Geng *et al.*, 2007; D'Angiolella *et al.*, 2013). The data also do not rule out the possibility that Cln3 carries out functions that are dependent upon Cdk1.

Cln3 influences protein levels of SCF^{Grr1} targets Hof1 and Ndd1

The available data can not explain how Cln3 influences Cln2 levels via post-transcriptional mechanisms, nor can the data explain how Cln3 influences the duration and extent of growth in mitosis. Furthermore, the fact that Cln3 does not show typical high affinity binding to Cdk1 suggests that it is necessary to consider models in which Cln3 carries out at least some functions independently of Cdk1. Together, these considerations suggest that a broad range of models for Cln3 function are possible. To illustrate the range of possible models, we consider here a model that arises from the observation that Cln3 binds to components of the SCF^{Grr1} ubiquitin ligase complex (Willems *et al.*, 1996; Landry *et al.*, 2012). Cln3 is thought to be a targeted for destruction by a combination of SCF^{Grr1} and SCF^{Cdc4} but the data do not rule out the possibility that Cln3 also regulates the SCF complex. Since SCF^{Grr1} targets Cln2 for destruction, these observations suggest a model in which Cln3 influences levels of Cln2 via regulation of the SCF complex. Since the SCF complex is likely to have a broad range of targets, Cln3-dependent regulation of the SCF complex could also explain how Cln3 influences the duration and extent of growth in mitosis. Previous work found that *cln3-Δ177* binds less effectively to components of the SCF^{Grr1} complex compared to full length Cln3 (Willems *et al.*, 1996; Landry *et al.*, 2012). Here, we found that *cln3-Δ177* also appeared to be less effective than full-length *CLN3* at causing increased levels of Cln2 protein, consistent with a model in which Cln3 binds and inhibits SCF^{Grr1} (compare **Figures 1B and 1D**). A full test of the model is beyond the scope of the current study, and additional details of the model are considered in the Discussion. Here, we tested whether protein levels of other known SCF^{Grr1} targets are influenced by loss or gain of function of Cln3. Two of the best characterized targets of SCF^{Grr1} are Hof1 and Ndd1. Hof1 controls cytokinesis, whereas Ndd1 is an essential transcription factor that controls expression of a cluster of mitotic genes that includes mitotic cyclins (Blondel *et al.*, 2005; Li *et al.*, 2006; Edenberg *et al.*, 2015). Both show strong cell cycle-dependent changes in protein levels.

We first analyzed Hof1-3XHA levels in asynchronous rapidly growing cells. Levels of Hof1 were decreased in *cln3Δ* cells and increased in *cln3-Δ177* cells (**Figure 7A**). In synchronized cells, *cln3-Δ177* led to an increase in Hof1 levels during mitosis, whereas *cln3Δ* led to a decrease in Hof1 levels (**Figure 7B**). We next compared the timing of expression of Hof1-3XHA and Cln3-6XHA in synchronized cells. Since the two proteins migrate at different locations in SDS-PAGE we were able to analyze levels of Hof1-3XHA and Cln3-6XHA in the same western blot. We also analyzed levels of the mitotic cyclin Clb2 as a marker for mitotic progression. Hof1-3XHA began to accumulate in early mitosis and reached peak levels late in mitosis, as levels of Clb2 began to decline (**Figure 7C**). Hof1 protein levels were strongly correlated with Cln3 protein levels, consistent with the possibility that Cln3 modulates levels of Hof1. The 6XHA tag used to detect Cln3 shows much higher sensitivity than the 3XHA tag used to detect Hof1, so relative levels of the two proteins cannot be compared.

We carried out a similar analysis for Ndd1. As with Hof1, *cln3Δ* caused a decrease in Ndd1 protein levels in both asynchronous and synchronous cells, whereas *cln3-Δ177* caused an increase in Ndd1 levels (**Figures 8A,B**). In contrast to Hof1, Ndd1 accumulates slightly before mitosis, consistent with its essential role in induction of transcription of mitotic cyclins and other mitotic genes. Therefore, Ndd1 levels are not closely correlated with Cln3 levels, and the effects of Cln3 on Ndd1 protein levels could be an indirect consequence of increased levels of late G1 cyclins, which are known to initiate mitotic transcription programs.

Previous studies have shown that loss of Hof1 causes a large increase in cell size, which suggests that decreased expression of Hof1 could contribute to the large size of *cln3Δ* cells.

However, the mechanisms by which Cln3 influences cell growth and size in mitosis remain largely unknown. At the least, these results demonstrate that loss of gain of function of Cln3 causes complex effects on the proteome that make it difficult to discern precisely how Cln3 influences cell size.

Discussion

Re-evaluation of the mechanisms that initiate cell cycle entry

It has been thought that Cln3/Cdk1 acts directly at SBF/MBF promoters to initiate transcription of late G1 cyclins (Costanzo *et al.*, 2004; de Bruin *et al.*, 2004; Skotheim *et al.*, 2008; Kõivomägi *et al.*, 2021). Cln3/Cdk1-dependent inactivation of Whi5 was initially thought to be a critical step in cell cycle entry; however, recent studies found no evidence for Cln3-dependent phosphorylation of Whi5 in vivo (Bhaduri *et al.*, 2015; Kõivomägi *et al.*, 2021), and genetic analysis has shown that Whi5 cannot be the sole target of Cln3 (Costanzo *et al.*, 2004; Wang *et al.*, 2009). Here, we found further evidence that suggests a need to re-evaluate the mechanisms that initiate cell cycle entry. First, we found that loss of Whi5 advances production of Cln2 protein but does not cause a general derepression of Cln2 protein expression, which indicates the existence of Whi5-independent mechanisms for repression of late G1 cyclin expression in early G1 phase. We also found that Cln3 can strongly influence the timing of Cln2 protein expression in *whi5*Δ cells. Furthermore, Cln2 protein expressed from a heterologous constitutive promoter still shows periodic expression in G1 phase that is strongly influenced by Cln3. Together, these observations suggest that post-transcriptional mechanisms play an important role in regulation of late G1 cyclin expression and function. These post-transcriptional mechanisms could play an important role in the steps that trigger cell cycle entry.

Cln3 does not show typical binding to Cdk1

Cln3 has been thought to exert it effects via binding and activation of Cdk1. Typical cyclins bind Cdk's so tightly that they form a stoichiometric complex that can be purified under conditions of high ionic strength (Kõivomägi *et al.*, 2011). However, no previous studies have found it possible to purify a stoichiometric Cln3-Cdk1 complex, which suggests that Cln3 binds Cdk1, at best, with a dramatically lower affinity than canonical cyclins. To circumvent the problem that a Cln3-Cdk1 complex can not be purified, a recent study expressed a Cln3-Cdk1 fusion protein in yeast (Kõivomägi *et al.*, 2021). The fusion protein could rescue the functions of G1 cyclins when Cdk1 expression is turned off; however, if Cln3 does not bind tightly to Cdk1 the Cln3-Cdk1 fusion protein could simply provide free Cdk1 that can be activated by Cln1 and Cln2, which are known to form a tight stoichiometric complex with Cdk1. Furthermore, biochemical assays utilizing the purified Cln3-Cdk1 fusion protein are complicated by the possibility that the Cdk1 in the Cln3-Cdk1 fusion could bind numerous other cyclins that co-purify with the fusion protein and influence assay results. Importantly, no studies have been able to show that purified Cln3 can bind and activate purified Cdk1. In the absence of this key biochemical test, it will remain unclear whether Cln3 can activate Cdk1.

Here, we used proteome-wide mass spectrometry to analyze the effects of loss or gain of function of Cln3, which found scant evidence that Cln3 is an important activator of Cdk1. Furthermore, we were unable to detect an interaction between Cln3 and Cdk1 in a co-immunoprecipitation assay. A small amount of Cdk1 could be detected in a GST-Cln3 pull down assay, as previously described (Bhaduri *et al.*, 2015); however, the amount of Cdk1 that was detected was 6-fold lower than the amount detected in a GST-Clb2 pulldown. Furthermore, we found evidence that the small amount of Cdk1 detected in Cln3 pull downs could be due to an indirect interaction. Multiple previous studies found that Cln3 binds SCF ubiquitin ligase complexes that also bind Cln1 and Cln2 (Willems *et al.*, 1996; Landry *et al.*, 2012). We detected Cln2 in GST-Cln3 pulldowns, which suggests that that Cln3 could bind Cln2/Cdk1 indirectly via a

complex that includes the SCF ubiquitin ligase, which would explain the small amount of Cdk1 in Cln3 pull-downs.

Taken together, the data thus far do not rule out the possibility that Cln3 carries out functions independently of Cdk1. In this case, Cln3 could be similar to mammalian cyclin F, which does not bind a Cdk (Bai *et al.*, 1994; D'Angiolella *et al.*, 2013). Cyclin E has also been proposed to carry out functions independently of Cdk activity (Geng *et al.*, 2007).

Swi6 is required for post-transcriptional control of Cln2 protein levels

We found that Swi6, the shared component of the SBF and MBF transcription factors, is required for the ability of Cln3 to modulate levels of Cln2 protein expressed from the *MET25* promoter. Interpretation of the phenotypes caused by *swi6*Δ is complicated by the fact that *swi6*Δ cells are barely viable and rapidly accumulate suppressors. In addition, SBF and MBF control the expression of hundreds of genes, including genes encoding multiple important transcription factors that have numerous targets involved in cell cycle regulation (i.e. Ndd1 and Hcm1), which indicates that *swi6*Δ will have pervasive and complex effects on the proteome (Iyer *et al.*, 2001; Horak *et al.*, 2002)). One potential explanation for the Swi6 requirement is that post-transcriptional regulation of Cln2 requires proteins expressed from genes controlled by SBF and MBF; however, the complex impacts of loss of Swi6 function make it difficult to define the responsible genes. Another potential explanation is that the Swi6 protein works directly in mechanisms that control translation or turnover of the Cln2 protein. For example, Swi6 could help serve as a platform for assembly of multiprotein complexes at promoters that control proteolytic turnover of late G1 cyclins. A role for Cln3 in regulating these kinds of complexes could explain the evidence that Cln3 associates with Swi6 and is found at SBF promoters (Wang *et al.*, 2009; Kõivomägi *et al.*, 2021).

Models for cell cycle entry

New data suggest a need to re-evaluate models for how Cln3 drives cell cycle entry. A broad range of models is possible. Here, we consider a model in which Cln3 promotes accumulation of late G1 cyclin via inhibition of the SCF^{Grr1} complex. This model arises from previous studies in which it was found that Cln3 binds to components of the SCF^{Grr1} complex, and that SCF^{Grr1} binds late G1 cyclins and targets them for destruction (Willems *et al.*, 1996; Skowyra *et al.*, 1997; Landry *et al.*, 2012). SCF^{Grr1} is thought to target Cln3 for destruction, but only after Cln3 has been phosphorylated on Cdk1 consensus sites (Landry *et al.*, 2012). In this case, unphosphorylated Cln3 that accumulates gradually during growth in G1 phase could inhibit SCF^{Grr1} to promote accumulation of active Cln2/Cdk1 complexes. Cln2 is thought to promote its own transcription in a positive feedback loop, (Cross and Tinkelenberg, 1991; Dirick and Nasmyth, 1991;Costanzo *et al.*, 2004; de Bruin *et al.*, 2004; Skotheim *et al.*, 2008; Wagner *et al.*, 2009). Therefore, an ability of Cln3 to promote accumulation of Cln2 could eventually allow Cln2/Cdk1 to engage the positive feedback loop, thereby initiating high level transcription of genes that drive cell cycle entry. Indeed, the data thus far do not rule out a model in which Cln3 promotes SBF-dependent transcription primarily via post-transcriptional mechanisms that drive an increase in Cln2 protein, which then engages the positive feedback loop (**Figure 9**). Once sufficient Cln2/Cdk1 accumulates it would target Cln3 for destruction, which would explain the decrease in Cln3 protein levels that occurs after cell cycle entry. This kind of model would suggest that the SCF complex plays an important role in repression of Cln2 protein expression in early G1 phase. The model is consistent with previously observed genetic interactions between genes that

influence cell cycle entry (Costanzo *et al.*, 2004; de Bruin *et al.*, 2004; Jorgensen and Tyers, 2004). Our discovery that Cln3 also influences levels of Hof1, another target of the SCF^{Grr1} complex, provides further support for the idea that Cln3 controls SCF^{Grr1}. Furthermore, our finding that Cln2 is present in GST-Cln3 pulldowns is consistent with the possibility that Cln3 binds and regulates a form of SCF^{Grr1} that targets Cln2 for destruction. The available data do not provide strong support for the model, but the data also do not exclude the model. Extensive biochemical analysis will be needed to distinguish models. In addition, the data do not rule out models in which Cln3 also works directly at SBF promoters to promote transcription of SBF-dependent genes, which would explain why Cln3 has been detected at SBF promoters (Wang *et al.*, 2009; Kõivomägi *et al.*, 2021).

Models for cell cycle entry must also explain how periodic expression of Cln2 protein is achieved in the absence of its normal transcriptional regulation, as observed here for Cln2 expressed from the heterologous *MET25* promoter. One explanation could be that Cln2/Cdk1 is capable of inhibiting SCF complexes when Cln2 protein levels reach a threshold, which would provide a positive feedback loop to drive accumulation of Cln2 as Cln3 levels rise (**Figure 9**). Similarly, the decline in Cln2 levels at the end of G1 phase could be explained if S phase cyclin/Cdk complexes stimulate SCF^{Grr1} to degrade Cln2.

The wide range of possible models for cell cycle entry has important implications. For example, it will not be possible to answer the critical question of how cell growth initiates cell cycle entry until we have a clear understanding of how cell cycle entry is initiated. Several recent studies suggested that growth-dependent accumulation of Cln3 initiates cell cycle entry and links cell cycle entry to cell growth (Litsios *et al.*, 2019; Sommer *et al.*, 2021)**.** This would be consistent with the model shown in **Figure 9**, where a threshold amount of Cln3 would drive sufficient accumulation of Cln2 to engage the positive feedback loop that triggers full transcription of late G1 cyclins and cell cycle entry.

Evidence for mitotic functions of Cln3 that influence cell size

Influential studies carried out over 50 years ago reached the conclusion that cell size is regulated primarily in G1 phase in budding yeast, and it has often been assumed that Cln3 exerts its effects on cell size solely in G1 phase (Hartwell and Unger, 1977). However, more recent work has shown that little growth occurs in G1 phase (Leitao and Kellogg, 2017). For example, cell volume increases by only 10-20% during G1 phase when cells are growing in rich nutrients. Rather, most growth of a budding yeast cell occurs as the daughter bud grows, which occurs almost entirely during mitosis (Leitao and Kellogg, 2017). Furthermore, the idea that Cln3 exerts all its effects on cell size in G1 phase is challenged by several observations. First, there is a second peak of Cln3 protein in mitosis, which suggests that Cln3 has functions in mitosis (Landry *et al.*, 2012; Zapata *et al.*, 2014; Litsios *et al.*, 2019). Second, analysis of Coulter Counter data shows that overexpression of Cln3 causes daughter cells to be born at a dramatically reduced size, which can only occur if daughter buds complete cell division at a smaller size (Costanzo *et al.*, 2004; Zapata *et al.*, 2014). These observations led us to hypothesize that Cln3 could influence cell size via effects on the duration and extent of bud growth in mitosis. To test this, we developed methods to induce conditional loss or gain of function of Cln3 after G1 phase and before mitosis, which showed that loss of Cln3 causes daughter cells to be born at a larger size, while overexpression of Cln3 causes them to be born at a smaller size. These data indicate that Cln3 can influence the duration and extent of bud growth in mitosis, and that mitotic functions of Cln3 can not be ignored when considering models for how Cln3 controls cell size.

The targets of Cln3 in mitosis that influence cell size are unknown. We found that Cln3 influences levels of Hof1, a mitotic regulator of cytokinesis, and that Hof1 protein levels in mitosis are correlated with Cln3 protein levels. These observations are consistent with the idea that Cln3 exerts important effects in mitosis. We and others have found that *hof1*Δ cells are larger than wild type cells, which suggests that part of the effects of Cln3 on cell size could be due to effects on Hof1 protein levels; however, Hof1 has not previously been implicated in cell size control and we found that overexpression of Hof1 does not reduce cell size. If it turns out that Cln3 regulates SCF activity, the effects of Cln3 on cell size could be the outcome of complex effects on multiple SCF targets.

Materials and Methods

Yeast strains, plasmids, media and cell cycle time courses.

All strains are in the W303 background and carry a deletion of the BAR1 gene to facilitate arrest with alpha factor (MATa *leu2-3,112 ura3-1 can1-100 ade2-1 his3-11,15 trp1-1 GAL+, ssd1-d2 bar1-*)]. The additional genetic features of the strains are listed in Table 3. Genetic alterations, such as epitope tagging, promoter swaps, and gene deletions were carried out using homologous recombination at the endogenous locus (Longtine *et al.*, 1998; Janke *et al.*, 2004).

Plasmid pAB1 was used to integrate *GAL1-CLN3-3XHA* at the *URA3* locus. To create pAB1, the GAL1 promoter was amplified and cloned into the KpnI and Xho1 sites of pRS306 (primers: CGCGGTACCTTATATTGAATTTTCAAAAATTCT and GCGCCTCGAGTATAGTTTTT-TTCTCCTTGACG) to make pDK20. A 3XHA tag sequence was then cloned into the EagI and SacII sites of pDK20 to create pSH32. The *CLN3* coding sequence was amplified and cloned into the XhoI and EagI sites of pSH32 (primers: GCGCTCGAGATGGCCATATTGAAGGATAC-CATAATTAGATACGC and CGCCGGCC-GGCGAGTTTTCTTGAGGTTGCTACTATC). pAB1 is cut with Stu1 to target integration at the URA3 locus.

For cell cycle time courses, cells were synchronized with 0.5 ug/ml alpha factor between 3-3.5 hours at room temperature and released from the arrest by washing cells 3 times with 25 mls of growth medium. For cell cycle time courses where *GAL1-CLN3* was induced, cells were grown in YP medium containing 2% glycerol and 2% ethanol (YPGE) and were arrested with alpha factor for 3.5-4 hours at room temperature. In Figure 5, *GAL1-CLN3* was induced by addition of 2% galactose at 60 minutes after release from alpha factor arrest. In Figure 1C and Figure 3, 2% galactose was added to the cultures 40 minutes before releasing from the arrest and cells were then released from the arrest into YP medium containing 2% galactose. All time courses were done at 30°C.

Cell size analysis

Cell size was measured with a Beckman Coulter Channelyzer Z2. Briefly, cells were grown in 10 mls culture medium to an OD_{600} between 0.4 - 0.6. Cells were then fixed by addition of 1/10 volume of formaldehyde for 30-60 minutes. Cells were pelleted and resuspended in 500 µl of PBS, 0.02% sodium azide and 0.1% Tween-20 and briefly sonicated. Cell size was measured using a Coulter Channelizer Z2; Beckman Coulter). In each Figure, cell size data represents the average of 3 biological replicates, in which each biological replicate is the average of 3 technical replicates.

Single cell analysis of cell growth and size during the cell cycle

Analysis of cell growth and size during the cell cycle was carried out as previously described (Leitao and Kellogg, 2017; Jasani *et al.*, 2020). Briefly, cells were grown in complete synthetic media (CSM) containing 2% dextrose (CSM-Dex) or 2% glycerol and 2% ethanol (CSM-G/E). For conditional expression of *GAL1-CLN3* 2% Galactose was added to the media when cells reached approximately 15% bud emergence, indicating that they were 20-30 minutes away from entering mitosis, which allowed sufficient time for expression *CLN3* from the *GAL1* promoter before mitosis. For conditional degradation of Cln3 in mitosis, auxin was added to the medium once cells were approximately 40-50% budded to allow for degradation of Cln3 before the beginning of mitosis. Sample preparation, data acquisition and processing was performed as previously described by (Leitao and Kellogg, 2017; Jasani *et al.*, 2020).

Mass spectrometry

Preparation of cell extracts: Cells (strains DK186, DK3099 and SH184) were grown overnight in 50 mls of YPD medium to OD_{600} between 0.4-0.5. 45 mls of culture were pelleted with a tabletop centrifuge for 1 minute at max speed and re-suspended in 1 ml of cold YPD medium. The resuspended pellet was then transferred to a 2 ml screw cap tube and the cells were pelleted again. The supernatant was removed and 200 µl of glass beads were added followed by freezing in liquid nitrogen. Frozen cells were lysed by bead-beating for 1 min using 300 µl of lysis buffer (8 M Urea, 75 mM NaCl, 50 mM Tris pH 8.2, 50 mM BGP, 1 mM Na_3VO_4, 10 mM Na_3PO_4, 1 mM PMSF) followed by 3 min centrifugation at 18,000xg in a microfuge at 4ºC. 200 µl of the supernatant was removed and transferred to a 1.5 ml tube. The pellet was then extracted again by adding another 300 µl lysis buffer, followed by a second round of bead-beating and centrifugation. The supernatants were combined and analyzed by mass spectrometry.

Protein extraction and digestion: Protein concentrations were determined using the bicinchoninic acid (BCA) assay (ThermoFisher Scientific). We precipitated 200 µg of protein using the estimated concentrations. Proteins were subjected to disulfide bond reduction with 5 mM tris (2-carboxyethyl) phosphine (room temperature, 15 min) and alkylation with 10 mM iodoacetamide (room temperature, 20 min in the dark). Excess iodoacetamide was quenched with 10 mM dithiotreitol (room temperature, 15 min in the dark). Methanol-chloroform precipitation was performed prior to protease digestion. In brief, 4 parts of neat methanol were added to each sample and vortexed, 1-part chloroform was added to the sample and vortexed, and 3 parts water was added to the sample and vortexed. The sample was centrifuged at 14,000 RPM for 2 min at room temperature and subsequently washed twice with 100% methanol. Samples were resuspended in 200 mM EPPS, pH 8.5 and digested at room temperature for 14 h with LysC protease at a 100:1 protein-to-protease ratio. Trypsin was then added at a 100:1 protein-to-protease ratio and the reaction was incubated for 6 h at 37°C.

Tandem mass tag labeling: TMT11 reagents (0.8 mg) were dissolved in anhydrous acetonitrile (40 µL) of which 5 µL was added to the peptides (50 µg) with 15 µL of acetonitrile to achieve a final concentration of approximately 30% (v/v). Following incubation at room temperature for 1 h, the reaction was quenched with hydroxylamine to a final concentration of 0.3% (v/v). TMT-labeled samples were pooled at a 1:1 ratio across all samples. For each experiment, the pooled sample was vacuum centrifuged to near dryness and subjected to C18 solid-phase extraction (SPE) (Sep-Pak, Waters).

Spin column-based phosphopeptide enrichment: Phosphopeptides were enriched from this pooled sample using the High-Select Fe-NTA Phosphopeptide Enrichment Kit (Paulo *et al.*, 2018). The only deviation from the manufacturer's protocol was that we prepared an "elution collection tube" with 100 µL of 10% formic acid into which the eluates were eluted. The combined eluate was vacuum centrifuged to near dryness and desalted via StageTip. The unbound and wash was used for Off-line basic pH reversed-phase BPRP fractionation to profile the proteome as described below.

Off-line basic pH reversed-phase (BPRP) fractionation: We fractionated the pooled TMT-labeled peptide sample via BPRP HPLC. We used an Agilent 1100 pump equipped with a degasser and a photodiode array (PDA) detector (set at 220 and 280 nm wavelength) from ThermoFisher Scientific (Waltham, MA). Peptides were subjected to a 50 min linear gradient from 5% to 35% acetonitrile in 10 mM ammonium bicarbonate pH 8 at a flow rate of 0.8 mL/min over an Agilent 300Extend C18 column (5 µm particles, 4.6 mm ID and 22 cm long). The peptide

mixture was fractionated into a total of 96 fractions, which were consolidated into 24 super-fractions, from which 12 non-adjacent samples were analyzed by mass spectrometry. These fractions were subsequently acidified with 1% formic acid and vacuum centrifuged to near dryness. Each fraction was also desalted via StageTip, dried via vacuum centrifugation, and reconstituted in 5% acetonitrile, 5% formic acid for LC-MS/MS processing.

Liquid chromatography and tandem mass spectrometry: Our mass spectrometry data were collected using an Orbitrap Fusion mass spectrometer (Thermo Fisher Scientific, San Jose, CA) coupled to a Proxeon EASY-nLC 1000 liquid chromatography (LC) pump (Thermo Fisher Scientific). Peptides were separated on a 100 µm inner diameter microcapillary column packed with ~35 cm of Accucore150 resin (2.6 µm, 150 Å, ThermoFisher Scientific, San Jose, CA). For each analysis, we loaded ~1 µg onto the column.

For protein level analysis, peptides were separated using a 150 min gradient of 3-24% acetonitrile in 0.125% formic acid at a flow rate of ~500 nL/min. Each analysis used the multi-notch MS3-based TMT method on an Orbitrap Fusion mass spectrometer. The scan sequence began with an MS1 spectrum (Orbitrap analysis; resolution 120,000; mass range 350-1400 m/z; automatic gain control (AGC) target 4.0E5; maximum injection time 50 ms). Precursors for MS2/MS3 analysis were selected using a Top10 method. Precursors were then selected for MS2/MS3 analysis (Ting *et al.*, 2011). MS2 analysis consisted of collision-induced dissociation (quadrupole ion trap analysis with turbo scan rate; AGC 1E4; normalized collision energy (NCE) 35; maximum injection time 60ms). MS3 precursors were fragmented by high energy collision-induced dissociation (HCD) and analyzed using the Orbitrap (NCE 65; AGC 1.5E5; maximum injection time 150 ms, resolution was 50,000).

For phosphopeptide level analysis, peptides were analyzed with three different methods (HCD, CID, CID-MSA). For all methods, peptides were separated using a 180 min gradient of 4-21% acetonitrile in 0.125% formic acid at a flow rate of ~500 nL/min. All analyses used the multi-notch MS3-based TMT method on an Orbitrap Fusion mass spectrometer. The scan sequence began with an MS1 spectrum (Orbitrap analysis; resolution 120,000; mass range 350-1400 m/z; automatic gain control (AGC) target 1.0E6; maximum injection time 50 ms). Precursors were then selected for MS2/MS3 analysis using a Top10 method (Huttlin *et al.*, 2010). The MS2 stage parameters differed for each of the three methods. For the HCD method, MS2 analysis consisted of collision-induced dissociation (quadrupole ion trap analysis with turbo scan rate; AGC 2E4; normalized collision energy (NCE) 32; maximum injection time 120ms). For the CID method, MS2 analysis consisted of collision-induced dissociation (quadrupole ion trap analysis with turbo scan rate; AGC 1E4; normalized collision energy (NCE) 35; maximum injection time 60ms). The CID-MSA method was identical to the CID method except that multistage activation (MSA) was enabled with a neutral loss mass of 97.9763. For all three modes of phosphopeptide analysis, MS3 precursors were fragmented by high energy collision-induced dissociation (HCD) and analyzed using the Orbitrap (NCE 65; AGC 1.5E5; maximum injection time 150 ms, resolution was 50,000).

Data analysis: Mass spectra were processed using a Sequest-based in-house software pipeline (Eng *et al.*, 1994). Spectra were converted to mzXML using a modified version of ReAdW.exe. Database searching included all entries from the *S. cerevisiae* UniProt database. The database was concatenated with one composed of all protein sequences for that database in the reversed order. Searches were performed using a 50-ppm precursor ion tolerance and a 1 Da product ion tolerance. These wide mass tolerance windows were chosen to maximize sensitivity in conjunction with Comet searches and linear discriminant analysis (Beausoleil *et al.*,

2006; Huttlin *et al.*, 2010). Carbamidomethylation of cysteine residues (+57.021 Da) was set as a static modification, while oxidation of methionine residues (+15.995 Da), and phosphorylation (+79.966, for the phosphopeptide-enriched samples) were set as variable modifications. PSMs (Peptide-spectrum matches) were adjusted to a 1% FDR (false discovery rate) (Elias and Gygi, 2007; Huttlin *et al.*, 2010). PSM filtering was performed using a linear discriminant analysis, as described previously (Huttlin *et al.*, 2010) and then assembled further to a final protein-level FDR of 1%.

Immunoprecipitation of Cln3 and Cln2

Protein A beads were prepared by washing 3X with wash buffer (50mM Hepes-KOH pH 7.6, 0.5 M KCl, 1 mM $MgCl_2$, 1 mM EGTA, 5% glycerol, 0.15% Tween-20) and incubating them overnight at 4°C with rabbit polyclonal anti-HA antibody. Cells (DK186, DK303 and DK3348) were grown overnight in 15 mls of YP medium containing 2% galactose to OD_{600} between 0.4-0.8. Cells were pelleted in tabletop centrifuge for 1 minute at max speed and re-suspended in 1 ml of growth medium. The resuspended pellet was then transferred to a 1.6 ml screw cap tube and the cells were pelleted again. After removal of the supernatant, 200 µl of glass beads were added and the cells were frozen in liquid nitrogen. 300 µl of extract buffer (50 mM Hepes-KOH pH 7.6, 0.5 M KCl, 1 mM $MgCl_2$, 1 mM EGTA, 5% glycerol, 0.15% Tween-20 containing 1 mM PMSF) was added to the frozen cells and the cells were lysed by bead-beating for 1 min in a Mini-beadbeater 16 (BioSpec). The extract was centrifuged for 3 min at 18,000xg in a microfuge at 4°C and 250 µl was removed to a 1.5 ml tube. The cells were then extracted again by adding 300 µl of extract buffer, followed by a second round of bead-beating and centrifugation. The supernatants were then combined and added to 20 ul of protein A beads with anti-HA antibody in a 0.6 ml tube. The anti-HA beads were mixed with extract on a rotator for 2 hours and were then washed 4 times with 400 ul of extract buffer followed by 2 washes with 1X Tris-Buffered saline with 0.1% Tween-20 detergent. After removal of the last supernatant, the beads were resuspended in 2X SDS-PAGE sample buffer and boiled 3 minutes before analyzing by SDS-PAGE and western blot.

GST-cyclin pulldowns

GST-cyclin pulldowns were carried out as previously described, with some minor modifications (Bhaduri *et al.*, 2015). Cells were grown overnight in -His + 2% G/E media to an OD_{600} between 0.4-0.6 and expression of GST fusion proteins was induced by addition of 2% galactose to the growth medium. Varying induction times were used to achieve similar expression levels of the GST-cyclin fusions. *GAL1-GST-CLB2* was induced for 30 minutes and *GAL1-GST*, *GAL1-GST-CLN310A* were induced for 90 minutes. Cells were pelleted in cold tabletop centrifuge for 5 minutes at max speed and washed 2X with 10 mls cold lysis buffer (25 mM Tris pH 7.5, 150 mM NaCl, 2 mM EDTA, 50 mM NaF, 10% glycerol). The pelleted cells were resuspended in 1 ml of lysis buffer and transferred to a 2 ml screw cap tube. The cells were pelleted again, the supernatant was removed, and the cell pellet was frozen in liquid nitrogen along with 400 µl of glass beads. Cells were lysed in 350 µl of lysis buffer containing 1 mM PMSF, 1mM DTT and 0.01% Triton X-100 by bead beating in a Mini-beadbeater 16 (BioSpec) at top speed for 1 min, chilled in an ice water bath for 30 seconds, beated again for 1 min, and chilled on ice for 30 sec. Additional Triton-X100 was added to bring final concentration to 0.5%. The cell lysate was mixed on a rotator for 10 min at 4°C and then pelleted at 18,000g for 1 min at max speed at 4ºC. The supernatant was transferred to 0.5 ml tube with 20 ul of glutathione-sepharose beads pre-equilibrated with lysis buffer, and tubes were mixed on a rotator for 1.5 hours at 4ºC. The beads

were washed 2X using 500 µl lysis buffer containing 0.01% Triton X-100, transferred to a new 1.6 ml screwcap tube and washed 3X using 500 µl lysis buffer containing 0.01% Triton X-100. After the last wash, 30 µl of 2X SDS-PAGE sample buffer was added and the beads were incubated in a boiling water bath for 5 minutes. 15 ul of each sample were analyzed by SDS-PAGE and western blot.

Cells that expressed *GAL1-CLN2-3XHA* in *GAL1-GST-CLB2*, *GAL1-GST* and *GAL1-GST-CLN310A* background were grown overnight to an OD_{600} between 0.6-0.8. Expression of *GAL1* promoter was induced with 2% galactose for 30 minutes in strain with *GAL1-CLN2-3XHA GAL1-GST-CLB2* and 90 minutes in *GAL1-CLN2-3XHA GAL1-GST*, *GAL1-CLN2-3XHA GAL1-CLN310A-GST* and *GAL1-CLN310A-GST*. 50 ml of cultures were collected after induction and cell pellets were obtained by spinning for 1 minute at 4,000 rpm. Cells were washed 2X with 10mls of lysis buffer (25 mM Tris pH 7.5, 500 mM NaCl, 2 mM EDTA, 50 mM NaF and 10% glycerol). The pelleted cells were resuspended in 1 ml of lysis buffer and transferred to a 2 ml screw cap tube to spin down for 30 seconds at max speed and aspirate supernatant to fast freeze in liquid nitrogen with 400 µl of glass beads. Cells were lysed in 350 µl of lysis buffer (25 mM Tris pH 7.5, 500 mM NaCl, 2 mM EDTA, 50 mM NaF and 10% glycerol) containing 1 mM PMSF, 1mM DTT and 0.01% Triton X-100 by bead beating as previously described. After cells were lysed and additional Triton-X100 was added to bring final concentration to 0.5%, cell lysate was run through a de-salting column for 2 minutes at 1000 rpm at 4ºC. Once cell lysate was collected after de-salting it was incubated with calibrated glutathione beads for 1 hour and 45 minutes. Samples were then prepared as previously described, beads were washed 2X using 500 µl lysis buffer containing 0.01% Triton X-100, transferred to a new 1.6 ml screwcap tube and washed 3X using 500 µl lysis buffer containing 0.01% Triton X-100. After the last wash, 30 µl of 2X SDS-PAGE sample buffer was added and the beads were incubated in a boiling water bath for 5 minutes. 15 ul of each sample were analyzed by SDS-PAGE and western blot.

Western Blotting

Western Blotting was done as previously described (Sommer et al., 2021). All polyacrylamide gels were 10% polyacrylamide and 0.13% bis-acrylamide, except for gels used for Cdk1 protein analysis, which were 12.5% polyacrylamide with 0.10% bis-acrylamide. All gels were transferred to a nitrocellulose membrane using Bio-Rad Trans-Blot Turbo Transfer system. Blots were probed overnight at 4°C in 3% dry milk in western wash buffer (PBS + 250 mM NaCl +0.1% Tween-20) using 12CA5 mouse monoclonal anti-HA, anti-Nap1, anti-Clb2, anti-GST or anti-Cdk1. Primary antibodies were detected with an HRP-conjugated donkey anti-rabbit secondary antibody or HRP-conjugated donkey anti-mouse secondary antibody as previously described by incubating for 1 hour at room temperature. Western blots were imaged using ECL reagents (K-12045-D50; Advansta) and a Bio-Rad Chemi-Doc Imaging system.

Western Blotting Quantification

All quantifications were done using Image Lab (Bio-Rad) as previously described (Jasani *et al.*, 2020; Sommer *et al.*, 2021). For alpha factor block and release experiments, the signal at each time point was calculated as a ratio over the signal at the 10-minute time point for the control strain. The signal for each time point was then normalized to the loading control. In Figure 6B, the Cdk1/cyclin ratio was calculated by dividing the signal for Cdk1 over the cyclin signal. For log phase samples, signals were calculated as a ratio over the WT control and then normalized to loading control.

Experimental Replicates: All experiments were repeated for a minimum of 3 biological replicates. Biological replicates are defined as experiments carried out on different days with cultures started with newly thawed cells.

Materials Availability: All yeast strains, plasmids and antibodies described in this study are available upon request.

Data Availability: All source data are included within the manuscript files.

Acknowledgements

This work was supported by NIH grant GM131826. A.B. supported by NIH grants GM058903 and GM133391, and by the ARCS Foundation, Marilyn D. Davis Memorial Scholarship, Denice Denton Award for Promoting Diversity, Café Bustelo El Café Del Futuro Scholarship, and UCSC Slug Support Office. We thank Benjamin Abrams (University of California, Santa Cruz) for providing technical support for the microscopy experiments, Peter Pryciak (University of Massachussets Medical School) for providing GAL1-GST-cyclin expression plasmids, and David Toczyski (University of California, San Francisco) for providing 12CA5 mouse monoclonal anti-HA antibody. We also thank Scott Rusin for providing technical support for mass spectrometry.

Citations

Andrews, BJ, and Herskowitz, I (1989). The yeast SWI4 protein contains a motif present in developmental regulators and is part of a complex involved in cell-cycle-dependent transcription. Nature 342, 830–833.

Andrews, BJ, and Moore, LA (1992). Interaction of the yeast Swi4 and Swi6 cell cycle regulatory proteins in vitro. Proc Natl Acad Sci 89, 11852–11856.

Bai, C, Richman, R, and Elledge, SJ (1994). Human cyclin F. EMBO J 13, 6087–6098.

Bean, JM, Siggia, ED, and Cross, FR (2005). High Functional Overlap Between MluI Cell-Cycle Box Binding Factor and Swi4/6 Cell-Cycle Box Binding Factor in the G1/S Transcriptional Program in *Saccharomyces cerevisiae*. Genetics 171, 49–61.

Beausoleil, SA, Villén, J, Gerber, SA, Rush, J, and Gygi, SP (2006). A probability-based approach for high-throughput protein phosphorylation analysis and site localization. Nat Biotechnol 24, 1285–1292.

Berset, C, Griac, P, Tempel, R, La Rue, J, Wittenberg, C, and Lanker, S (2002). Transferable Domain in the G1 Cyclin Cln2 Sufficient To Switch Degradation of Sic1 from the E3 Ubiquitin Ligase SCFCdc4 to SCFGrr1. Mol Cell Biol 22, 4463–4476.

Bhaduri, S, Valk, E, Winters, MJ, Gruessner, B, Loog, M, and Pryciak, PM (2015). A Docking Interface in the Cyclin Cln2 Promotes Multi-site Phosphorylation of Substrates and Timely Cell-Cycle Entry. Curr Biol 25, 316–325.

Blondel, M, Bach, S, Bamps, S, Dobbelaere, J, Wiget, P, Longaretti, C, Barral, Y, Meijer, L, and Peter, M (2005). Degradation of Hof1 by SCFGrr1 is important for actomyosin contraction during cytokinesis in yeast. EMBO J 24, 1440–1452.

de Bruin, RAM, McDonald, WH, Kalashnikova, TI, Yates, J, and Wittenberg, C (2004). Cln3 Activates G1-Specific Transcription via Phosphorylation of the SBF Bound Repressor Whi5. Cell 117, 887–898.

Carter, BLA, and Sudbery, PE (1980). Small-Sized Mutants of Saccharomyces Cerevisiae. Genetics 96, 561–566.

Costanzo, M, Nishikawa, JL, Tang, X, Millman, JS, Schub, O, Breitkreuz, K, Dewar, D, Rupes, I, Andrews, B, and Tyers, M (2004). CDK Activity Antagonizes Whi5, an Inhibitor of G1/S Transcription in Yeast. Cell 117, 899–913.

Cross, FR (1988). DAF1, a mutant gene affecting size control, pheromone arrest, and cell cycle kinetics of Saccharomyces cerevisiae. Mol Cell Biol 8, 4675–4684.

Cross, FR (1989). Further characterization of a size control gene in *Saccharomyces cerevisiae*. J Cell Sci 1989, 117–127.

Cross, FR (1990). Cell cycle arrest caused by CLN gene deficiency in Saccharomyces cerevisiae resembles START-I arrest and is independent of the mating-pheromone signalling pathway. Mol Cell Biol 10, 6482–6490.

D'Angiolella, V, Esencay, M, and Pagano, M (2013). A cyclin without CDKs: Cyclin F controls genome stability through ubiquitin-mediated proteolysis. Trends Cell Biol 23, 135–140.

Di Talia, S, Wang, H, Skotheim, JM, Rosebrock, AP, Futcher, B, and Cross, FR (2009). Daughter-Specific Transcription Factors Regulate Cell Size Control in Budding Yeast. PLoS Biol 7, e1000221.

Edenberg, ER, Mark, KG, and Toczyski, DP (2015). Ndd1 Turnover by SCFGrr1 Is Inhibited by the DNA Damage Checkpoint in Saccharomyces cerevisiae. PLOS Genet 11, e1005162.

Elias, JE, and Gygi, SP (2007). Target-decoy search strategy for increased confidence in large-scale protein identifications by mass spectrometry. Nat Methods 4, 207–214.

Eng, JK, McCormack, AL, and Yates, JR (1994). An approach to correlate tandem mass spectral data of peptides with amino acid sequences in a protein database. J Am Soc Mass Spectrom 5, 976–989.

Ferrezuelo, F, Colomina, N, Futcher, B, and Aldea, M (2010). The transcriptional network activated by Cln3 cyclin at the G1-to-S transition of the yeast cell cycle. Genome Biol 11, R67.

Geng, Y, Lee, Y-M, Welcker, M, Swanger, J, Zagozdzon, A, Winer, JD, Roberts, JM, Kaldis, P, Clurman, BE, and Sicinski, P (2007). Kinase-Independent Function of Cyclin E. Mol Cell 25, 127–139.

Hadwiger, JA, Wittenberg, C, Richardson, HE, de Barros Lopes, M, and Reed, SI (1989). A family of cyclin homologs that control the G1 phase in yeast. Proc Natl Acad Sci U S A 86, 6255–6259.

Hartwell, LH, and Unger, MW (1977). Unequal division in Saccharomyces cerevisiae and its implications for the control of cell division. J Cell Biol 75, 422–435.

Horak, CE, Luscombe, NM, Qian, J, Bertone, P, Piccirrillo, S, Gerstein, M, and Snyder, M (2002). Complex transcriptional circuitry at the G1/S transition in Saccharomyces cerevisiae. Genes Dev 16, 3017–3033.

Huttlin, EL, Jedrychowski, MP, Elias, JE, Goswami, T, Rad, R, Beausoleil, SA, Villén, J, Haas, W, Sowa, ME, and Gygi, SP (2010). A tissue-specific atlas of mouse protein phosphorylation and expression. Cell 143, 1174–1189.

Iyer, VR, Horak, CE, Scafe, CS, Botstein, D, Snyder, M, and Brown, PO (2001). Genomic binding sites of the yeast cell-cycle transcription factors SBF and MBF. Nature 409, 533–538.

Janke, C et al. (2004). A versatile toolbox for PCR-based tagging of yeast genes: new fluorescent proteins, more markers and promoter substitution cassettes. Yeast 21, 947–962.

Jasani, A, Huynh, T, and Kellogg, DR (2020). Growth-Dependent Activation of Protein Kinases Suggests a Mechanism for Measuring Cell Growth. Genetics 215, 729–746.

Jorgensen, P, Nishikawa, JL, Breitkreutz, B-J, and Tyers, M (2002). Systematic Identification of Pathways That Couple Cell Growth and Division in Yeast. Science 297, 395–400.

Jorgensen, P, and Tyers, M (2004). How Cells Coordinate Growth and Division. Curr Biol 14, R1014–R1027.

Kishi, T, and Yamao, F (1998). Grr1 links Cln2 to Skp1 during Cln2 degradation. J Cell Sci, 111 (Pt 24):3655-61.

Koch, C, Schleiffer, A, Ammerer, G, and Nasmyth, K (1996). Switching transcription on and off during the yeast cell cycle: Cln/Cdc28 kinases activate bound transcription factor SBF (Swi4/Swi6) at start, whereas Clb/Cdc28 kinases displace it from the promoter in G2. Genes Dev 10, 129–141.

Kõivomägi, M, Swaffer, MP, Turner, JJ, Marinov, G, and Skotheim, JM (2021). Localized phosphorylation of RNA Polymerase II by G1 cyclin-Cdk promotes cell cycle entry, Cell Biology.

Kõivomägi, M, Valk, E, Venta, R, Iofik, A, Lepiku, M, Morgan, DO, and Loog, M (2011). Dynamics of Cdk1 Substrate Specificity during the Cell Cycle. Mol Cell 42, 610–623.

Landry, BD, Doyle, JP, Toczyski, DP, and Benanti, JA (2012). F-Box Protein Specificity for G1 Cyclins Is Dictated by Subcellular Localization. PLoS Genet 8, e1002851.

Leitao, RM, and Kellogg, DR (2017). The duration of mitosis and daughter cell size are modulated by nutrients in budding yeast. J Cell Biol 216, 3463–3470.

Li, WJ, Wang, YM, Zheng, XD, Shi, QM, Zhang, TT, Bai, C, Li, D, Sang, JL, and Wang, Y (2006). The F-box protein Grr1 regulates the stability of Ccn1, Cln3 and Hof1 and cell morphogenesis in Candida albicans. Mol Microbiol 62, 212–226.

Litsios, A et al. (2019). Differential scaling between G1 protein production and cell size dynamics promotes commitment to the cell division cycle in budding yeast. Nat Cell Biol 21, 1382–1392.

Longtine, MS, Iii, AM, Demarini, DJ, Shah, NG, Wach, A, Brachat, A, Philippsen, P, and Pringle, JR (1998). Additional modules for versatile and economical PCR-based gene deletion and modification in Saccharomyces cerevisiae. Yeast 14, 953–961.

Miller, ME, Cross, FR, Groeger, AL, and Jameson, KL (2005). Identification of novel and conserved functional and structural elements of the G1 cyclin Cln3 important for interactions with the CDK Cdc28 inSaccharomyces cerevisiae. Yeast 22, 1021–1036.

Nash, R, Tokiwa, G, Anand, S, Erickson, K, and Futcher, AB (1988). The WHI1+ gene of Saccharomyces cerevisiae tethers cell division to cell size and is a cyclin homolog. EMBO J 7, 4335–4346.

Nasmyth, K (1993). Control of the yeast cell cycle by the Cdc28 protein kinase. Curr Opin Cell Biol 5, 166–179.

Nasmyth, K, and Dirick, L (1991). The Role of SW4 and SW16 in the Activity of Gl Cyclins in Yeast. 19.

Nishimura, K, Fukagawa, T, Takisawa, H, Kakimoto, T, and Kanemaki, M (2009). An auxin-based degron system for the rapid depletion of proteins in nonplant cells. Nat Methods 6, 917–922.

Paulo, JA, Navarrete-Perea, J, Erickson, AR, Knott, J, and Gygi, SP (2018). An Internal Standard for Assessing Phosphopeptide Recovery from Metal Ion/Oxide Enrichment Strategies. J Am Soc Mass Spectrom 29, 1505–1511.

Richardson, HE, Wittenberg, C, and Cross, F (1989). An Essential Gl Function for Cyclin-like Proteins in Yeast. 7.

Schneider, BL, Zhang, J, Markwardt, J, Tokiwa, G, Volpe, T, Honey, S, and Futcher, B (2004). Growth Rate and Cell Size Modulate the Synthesis of, and Requirement for, G1-Phase Cyclins at Start. Mol Cell Biol 24, 10802–10813.

Siegmund, RF, and Nasmyth, KA (1996). The Saccharomyces cerevisiae Start-specific transcription factor Swi4 interacts through the ankyrin repeats with the mitotic Clb2/Cdc28 kinase and through its conserved carboxy terminus with Swi6. Mol Cell Biol 16, 2647–2655.

Skotheim, JM, Di Talia, S, Siggia, ED, and Cross, FR (2008). Positive feedback of G1 cyclins ensures coherent cell cycle entry. Nature 454, 291–296.

Skowyra, D, Craig, KL, Tyers, M, Elledge, SJ, and Harper, JW (1997). F-Box Proteins Are Receptors that Recruit Phosphorylated Substrates to the SCF Ubiquitin-Ligase Complex. Cell 91, 209–219.

Sommer, RA, DeWitt, JT, Tan, R, and Kellogg, DR (2021). Growth-dependent signals drive an increase in early G1 cyclin concentration to link cell cycle entry with cell growth. ELife 10, e64364.

Spellman, PT, Sherlock, G, Zhang, MQ, Anders, K, Eisen, MB, Brown, PO, and Futcher, B (1998). Comprehensive Identification of Cell Cycle–regulated Genes of the Yeast Saccharomyces cerevisiae by Microarray Hybridization□D. Mol Biol Cell 9, 25.

Sudbery, PE, Goodey, AR, and Carter, BLA (1980). Genes which control cell proliferation in the yeast Saccharomyces cerevisiae. Nature 288, 401–404.

Ting, L, Rad, R, Gygi, SP, and Haas, W (2011). MS3 eliminates ratio distortion in isobaric labeling-based multiplexed quantitative proteomics. Nat Methods 8, 937–940.

Tyers, M, Tokiwa, G, and Futcher, B (1993). Comparison of the Saccharomyces cerevisiae G1 cyclins: Cln3 may be an upstream activator of Cln1, Cln2 and other cyclins. EMBO J 12, 1955–1968.

Tyers, M, Tokiwa, G, Nash, R, and Futcher, B (1992). The Cln3-Cdc28 kinase complex of S. cerevisiae is regulated by proteolysis and phosphorylation. EMBO J 11, 1773–1784.

Wagner, MV, Smolka, MB, de Bruin, RAM, Zhou, H, Wittenberg, C, and Dowdy, SF (2009). Whi5 Regulation by Site Specific CDK-Phosphorylation in Saccharomyces cerevisiae. PLoS ONE 4, e4300.

Wang, H, Carey, LB, Cai, Y, Wijnen, H, and Futcher, B (2009). Recruitment of Cln3 Cyclin to Promoters Controls Cell Cycle Entry via Histone Deacetylase and Other Targets. PLoS Biol 7, e1000189.

Wijnen, H, Landman, A, and Futcher, B (2002). The G1 Cyclin Cln3 Promotes Cell Cycle Entry via the Transcription Factor Swi6. Mol Cell Biol 22, 4402–4418.

Willems, AR, Lanker, S, Patton, EE, Craig, KL, Nason, TF, Mathias, N, Kobayashi, R, Wittenberg, C, and Tyers, M (1996). Cdc53 Targets Phosphorylated G1 Cyclins for Degradation by the Ubiquitin Proteolytic Pathway. Cell 86, 453–463.

Zapata, J, Dephoure, N, MacDonough, T, Yu, Y, Parnell, EJ, Mooring, M, Gygi, SP, Stillman, DJ, and Kellogg, DR (2014). PP2ARts1 is a master regulator of pathways that control cell size. J Cell Biol 204, 359–376.

Figure Legends

Figure 1: **Cln3 can influence production of Cln2 protein via Whi5-independent mechanisms**
(A) Cells were grown in YPD medium overnight and synchronized in G1 phase using alpha factor. Cells were released from G1 arrest and samples were collected every 10 minutes to assay for Cln2-3XHA protein levels by western blotting using 12CA5 mouse monoclonal anti-HA. An anti-Nap1 antibody was used as the loading control. **(B)** Quantification of data in panel A. Cln2 protein levels were normalized against loading control. Error bars represent the standard error of the mean for 3 biological replicates. **(C)** Cells were grown in 2% YPGE medium overnight and synchronized in G1 phase using mating pheromone. 2% galactose was added to cultures at 40 minutes prior to release from G1 arrest. Cells were released from G1 arrest into YP medium containing 2% galactose and samples were collected every 10 minutes to assay for Cln2 protein levels by western blotting using 12CA5 mouse monoclonal anti-HA. **(D)** Quantification of data in panel C. Error bars represent standard error of the mean for 3 biological replicates.

Figure 2: Cln3 can influence levels of Cln2 protein via post-transcriptional mechanisms
(A) Cells were grown in YPD medium overnight and synchronized in G1 phase using alpha factor. Cells were released from G1 arrest and samples were collected every 10 minutes to assay for MET25-3XHA-Cln2 protein levels by western blotting using 12CA5 mouse monoclonal anti-HA. An anti-Nap1 antibody was used as the loading control. **(B)** Quantification of the data in panel A. Plots were generated by normalizing MET25-3XHA-CLN2 to loading control. Error bars represent the standard error of the mean for 4 biological replicates.

Figure 3: Cln3 requires Swi6 to influence Cln2 protein levels
(A,B) Cells were grown in YPGE medium overnight and synchronized in G1 phase using alpha factor. 2% galactose was added to the cultures 40 minutes prior to release from G1 arrest. Cells were released from G1 arrest into YP medium containing 2% galactose and samples were collected every 10 min. Western blotting was used to assay protein levels for Cln2 using 12CA5 mouse monoclonal anti-HA **(A)** and Clb2 using an anti-Clb2 antibody **(B)**.

Figure 4: Cln3 can influence cell size via mechanisms that are independent of transcriptional control of Cln1 and Cln2
(A, B) Cells were grown in YPD medium or YP medium containing 2% galactose overnight to an OD_{600} between 0.4 - 0.6 and cell size was measured using a Beckman Coulter Channelizer Z2. Data shown represents the average of 3 biological replicates, where each biological replicate is the average of 3 technical replicates.

Figure 5: Cln3 carries out functions in mitosis that influence cell size
Mitotic spindle poles in wild type control cells were labelled with Spc42-mRUBY2, whereas the mitotic spindle poles of *GAL1-CLN3* or *cln3-AID* cells were labeled with Spc42-eGFP. For experiments comparing wild type to *GAL1-CLN3*, cells were grown in complete synthetic media (CSM) containing 2% glycerol and 2% ethanol overnight. The cells were then arrested in G1 phase using alpha factor and wild type and mutant cells were mixed before releasing from the arrest. Cells were released in CSM containing 2% glycerol/ethanol and 2% galactose was added 60 minutes after release. For experiments comparing wild type cells to *cln3-AID*, cells were grown overnight in CSM containing 2% dextrose and were arrested in G1 phase using alpha factor. The wild type and mutant cells were mixed before releasing from the G1 phase arrest. 0.5 mM auxin was added at 50 minutes after release. Cells were imaged by confocal microscopy at 3-minute intervals at a constant temperature of 27°C. **(A)** Graphs comparing the duration of each stage of

mitosis in wild type and *GAL1-CLN3* cells. **(B)** Graphs comparing bud volume at the end of metaphase and the end of mitosis in wild type and *GAL1-CLN3* cells. **(C)** Graphs comparing the duration of each stage of mitosis in wild type and *cln3-AID* cells. **(D)** Graphs comparing bud volume at the end of metaphase and the end of mitosis in wild type and *cln3-AID* cells. Bars indicate the mean and the standard error of the mean for n=29 (wild type, *GAL1CLN3*) in panels A and B, and n=49 (wild type) and n=45 (*cln3-AID)* in panels C and D.

Figure 5, figure supplement: Cell size analysis of *cln3-AID* cells.
Cells were grown overnight in YPD medium containing either 0.5 mM auxin or an ethanol solvent control. Cell size was measured using a Coulter counter. Data shown represents the average of 3 biological replicates, in which each biological replicate represents the average of 3 technical replicates.

Figure 6: Cln3 does not show typical binding to Cdk1
(A) Wild type, *GAL1-CLB2-3XHA* and *GAL1-CLN3-3XHA* cells were grown in YP medium containing 2% galactose overnight to an OD_{600} between 0.4 - 0.6. Cells were lysed and Clb2-3XHA and Cln3-3XHA were immunoprecipitated with an anti-HA polyclonal antibody. Cdk1 was detected with an anti-Cdk1 rabbit polyclonal antibody. **(B)** Cells were grown overnight in CSM -His medium containing 2% glycerol and 2% ethanol to an OD_{600} between 0.4 - 0.6. *GAL1-GST-CLB2* was induced with 2% galactose for 30 minutes and *GAL1-GST*, *GAL1-GST-CLN3-10A* were induced for 90 minutes. Cells were lysed and the GST fusion proteins were purified using glutathione beads. The fusion protein was detected with an anti-GST rabbit polyclonal antibody and Cdk1 was detected with an anti-Cdk1 rabbit polyclonal antibody. **(C)** Cells were grown overnight in CSM -His medium containing 2% glycerol and 2% ethanol to an OD_{600} between 0.6 - 0.8. before induction of expression from the *GAL1* promoter. GST fusion proteins were purified using glutathione beads as described in the Methods, and proteins were detected by western blot using anti-GST rabbit polyclonal, anti-Cdk1 rabbit polyclonal and monoclonal 12CA5 mouse monoclonal anti-HA antibodies.

Figure 7: Cln3 influences levels of Hof1 protein
(A) Western blots showing levels of Hof1 protein in asynchronous wt, *cln3*Δ, and *cln3-Δ177* cells. Bar graphs show quantification of three biological replicates. Error bars show standard error of the mean. **(B)** Cells were grown overnight in YPD medium and synchronized in G1 phase using alpha factor. Cells were released from G1 arrest and samples were collected every 10 minutes. The behavior of Hof1-3XHA was assayed by western blot using 12CA5 mouse monoclonal anti-HA. An anti-Nap1 antibody served as a loading control. The graph shows quantification of data from three biological replicates normalized to loading control. Error bars represent the standard error of the mean. **(C)** Wild type cells containing Cln3-6XHA and Hof1-3XHA were grown overnight in YPD medium and sychronized in G1 phase with alpha factor. After release from the G1 arrest, the behavior of Cln3-6XHA and Hof1-3XHA was assayed by western blot using 12CA5 mouse monoclonal anti-HA.

Figure 8: Cln3 influences levels of Ndd1 protein
(A) Western blots showing levels of Ndd1 protein in asynchronous wt, *cln3*Δ, and *cln3-Δ177* cells using 12CA5 mouse monoclonal anti-HA. Bar graphs show quantification of three biological replicates normalized to loading control. Error bars show standard error of the mean. **(B)** Cells were grown overnight in YPD medium and synchronized in G1 phase using alpha factor. Cells were released from G1 arrest and samples were collected every 10 minutes. The behavior of Ndd1-3XHA was assayed by western blot. An anti-Nap1 antibody served as a loading control. The graph shows quantification of data from three biological replicates. Error bars represent the standard error of the mean.

Figure 9: Proposed Model
A potential model for regulation of cell cycle entry.

Source Data:
Figure 1 source data: Original unprocessed western blots for Figure 1, panels A,C.
Figure 2 source data: Original unprocessed western blots for Figure 2, panel A.
Figure 3 source data: Original unprocessed western blots for Figure 3, panels A,B
Figure 6 source data: Original unprocessed western blots for Figure 6, panels A,B,C
Figure 7 source data: Original unprocessed western blots for Figure 7, panels A,B,C
Figure 8 source data: Original unprocessed western blots for Figure 8, panels A,B

Table 1. Peptides that undergo loss in phosphorylation in *cln3*Δ cells.
A list of peptides that showed a greater than 2-fold loss of phosphorylation in *cln3*Δ cells. Phosphorylation sites that also showed any gain of phosphorylation in *cln3-Δ177* cells are highlighted in yellow. Proteins that yielded peptides with minimal Cdk1 consensus sites that showed loss of phosphorylation in *cln3*Δ cells and gain of phosphorylation in *cln3-Δ177* cells are highlighted in green.

Gene symbol	Site Position	Motif	Sequence	*cln3*Δ/WT log2	*cln3-Δ177*/WT log2
CHS2	225	SKRRMVSDLPPPS	R.MVS#DLPPPSK.K	-1.657238285	0.107693645
RSN1	931	ANGEFDTASKENN	K.DEANGEANGEFDT#AS#K.E	-1.441783557	0.509619257
RSN1	931;933	ANGEFDTASKENN;GEFDTASKENNPF	K.DEANGEANGEFDT#AS#K.E	-1.441783557	0.509619257
BDP1	134	RSSRLASLSKDNE	R.LAS#LSK.D	-1.269386916	0.402038618
ROX1	366	AKTSLVSPKxxxx	K.TSLVS#PK.-	-1.265376151	0.499047778
TOS4	65	SIGRVSSPVRSNK	R.VSS#PVR.S	-1.257505978	0.643833503
BOI1	637;640	HARSQSYSHSRKH;SQSYSHSRKHSLV	R.SQS#YSHS#R.K	-1.179550343	0.141433426
ZRT2	188	NEEIVATPIKEKE	R.NEEIVAT#PIK.E	-1.178661842	-0.218949928
RFA1	160	VPDMLHSNSNLNA	K.DEDITDSGNVANQTNASNAGVPDMLHS#NSNLNANER.K	-1.167843779	0.795326087
BOI1	637	HARSQSYSHSRKH	R.SQS#Y#SHSR.K	-1.158609504	0.159994972
NOP16	176	VIRKERSQSEREE	K.ERS#QSEREEEWLEK.L	-1.135146671	0.647447925
DIP5	22	NSSSLDSDHDAYY	K.MFTSTS#PRNS#SSLDS#DHDAYYSK.Q	-1.123554019	-0.112368825
AIM3	729	IRKRAPTPPAPSR	K.RAPT#PPAPSR.S	-1.117599707	-0.525199157
TRM8	7	MKAKPLSQDPGSK	K.AKPLS#QDPGSK.R	-1.106220562	0.817875558
BOI1	636	SHARSQSYSHSRK	R.SQS#Y#SHSR.K	-1.101760827	0.210537023
BOI1	636;637	SHARSQSYSHSRK;HARSQSYSHSRKH	R.SQS#Y#SHSR.K	-1.101760827	0.210537023
BOI1	86	PENLHKSPTQESG	K.S#PTQESGNSGVK.Y	-1.086312554	0.047693299
FIN1	68	KHSIQVTPRRIMS	K.HSIQVT#PR.R	-1.060470569	0.600358622
YDR348C	216	HREASSSSTPSKK	R.EASS#S#ST#PSK.K	-1.039225105	0.667444024
YDR348C	214;216;218	HHHREASSSSTPS;HREASSSSTPSKK;EASSSSTPSKKGK	R.EASS#S#ST#PSK.K	-1.039225105	0.667444024
RSN1	933	GEFDTASKENNPF	K.DEANGEANGEFDT#AS#K.E	-1.037786427	0.441066753
AXL2	754	NIQDSQSGKNGIT	R.HLQNIQDSQS#GK.N	-1.035769076	0.248194484
HTB2	129	TKYSSSTQAxxxx	K.YSSST#QA.-	-1.032539872	1.2076134
DIP5	13	KMFTSTSPRNSSS	K.MFTSTS#PR.N	-1.02737546	-0.16685546
NUP60	480;483	VQKKSRSNLSQEN;KSRSNLSQENDNE	K.SRS#NLS#QENDNEGK.H	-1.021434117	0.147293213
SPC29	191	EHSRSFSGFPTNK	R.SFS#GFPTNK.T	-1.020182957	0.559835141
MIA40	356	EQLKETSDDEEPQ	K.ETS#DDEEPQDK.V	-1.015734149	0.754376195
BOI1	578	GHSRDASLSEMKK	R.DAS#LSEMK.K	-1.000525238	0.255793359

Table 2. Peptides that undergo increase in phosphorylation in *cln3-Δ177* cells

A list of peptides that showed a greater than 2-fold gain of phosphorylation in *cln3-Δ177* cells. Phosphorylation sites that also showed any loss of phosphorylation in *cln3Δ* cells are highlighted in yellow. Proteins that yielded peptides with minimal Cdk1 consensus sites that showed gain of phosphorylation in *cln3-Δ177* cells and loss of phosphorylation in *cln3Δ* cells are highlighted in green.

Gene symbol	Site Position	Motif	Sequence	*cln3Δ* /WT log2	*cln3-Δ177* /WT log2
MRH1	295	SPRPAATPNLSKD	K.APVAS#PRPAAT#PNLSK.D	1.031841117	1.654001672
DDR48	293	SSNDDSYGSSNND	K.SSYGSSSNDDSY#GS#SNNDDSYGSSNK.K	-0.200749844	1.552460834
DDR48	293;295	SSNDDSYGSSNND;NDDSYGSSNNDDS	K.SSYGSSSNDDSY#GS#SNNDDSYGSSNK.K	-0.200749844	1.552460834
RPL12B	38	IGPLGLSPKKVGE	K.IGPLGLS#PKK.V	-0.947943715	1.504893267
DDR48	189	SNNDDSYGSNNDD	K.SSYGSNNDDSY#GS#NNDDSYGSSNK.K	-0.371162019	1.41604204
DDR48	189;191	SNNDDSYGSNNDD;NDDSYGSNNDDSY	K.SSYGSNNDDSY#GS#NNDDSYGSSNK.K	-0.371162019	1.41604204
IES5	124	LYNDTHTPxxxxx	K.ETPLLYNDTHT#P.-	0.08210317	1.31262001
MRH1	289	PKAPVASPRPAAT	K.APVAS#PRPAAT#PNLSK.D	0.918047331	1.246420723
DDR48	191	NDDSYGSNNDDSY	K.SSYGSNNDDSYGS#NNDDSYGSSNK.K	-0.241590167	1.234618569
ASH1	253	RSSKFHSPSKESF	K.FHS#PSK.E	-0.040912948	1.231379863
HTB2	129	TKYSSSTQAxxxx	K.YSSST#QA.-	-1.032539872	1.2076134
NUP60	483	KSRSNLSQENDNE	K.SRS#NLS#QENDNEGK.H	-0.721678187	1.190002553
HXT3	13;23	LISPQKSSENSNA;SNADLPSNSSQVM	K.SS#ENSNADLPS#NSSQVMNMPEEK.G	-0.264612633	1.183330198
SNF2	383	SQTVSGTPITQTE	K.NSQTVSGT#PITQTESK.K	-0.641366992	1.174179922
DDR48	217	NNDSYGSNNDDSY	K.SSYGSSNNDSYGS#NNDDSYGSNNNDSYGSNNDDSYGSSNK.K	-0.12756302	1.143978954
NOP10	36	AHPARFSPDDKYS	R.FS#PDDK.Y	-0.182030806	1.142662436
ACE2	259	SPVILKTPAMQNG	K.T#PAM*QNGR.M	0.269982679	1.133745736
YMR196W	1013;1017	GTHSGLTPQSSIS;GLTPQSSISSDKA	R.IGGTHSGLT#PQSS#ISSDK.A	1.731714916	1.125759472
DDR48	238	GSNNDDSYGSSNK	K.SSYGSSNNDSYGSNNDDSYGS#NNNDSYGSNNDDS#YGSSNK.K	-0.46965693	1.110258313
DDR48	217;238	NNDSYGSNNDDSY;GSNNDDSYGSSNK	K.SSYGSSNNDSYGSNNDDSYGS#NNNDSYGSNNDDS#YGSSNK.K	-0.46965693	1.110258313
DLS1	17	ASAPLCSPKLPVE	K.ETASAPLCS#PK.L	-0.563081699	1.100106082
SPP41	393	ASTANKSPASEST	K.S#PASESTSK.K	-0.506239873	1.090562292
CLC1	52	ILETEASPAKDDD	K.TEQDDILETEAS#PAK.D	0.634857175	1.090505649
CAF120	524	SPHKVHTPTDASF	K.VHT#PTDASFR.T	-0.178758197	1.080266415
RAD23	101;106	PGRENSTEASPST;STEASPSTDASAA	R.ENST#EAS#PSTDASAAPAATAPEGSQPQEEQTATTER.T	0.225374102	1.052755574
DDR48	248	SNKKKSSYGSNND	K.KSS#Y#GSNNDDSYGSSNNNDSYGSNNDDSYGSSNK.N	-0.201649568	1.04525593
DDR48	248;257	SNKKKSSYGSNND;SNNDDSYGSSNNN	K.KSS#Y#GSNNDDSYGSSNNNDSYGSNNDDSYGSSNK.N	-0.201649568	1.04525593
RPS28B	5	xxMDSKTPVTLAK	K.T#PVTLAK.V	0.161710152	1.042847748
SPC110	36	TQTQVVSPTKVPN	K.RNTTQTQVVS#PTK.V	-0.60010086	1.022129821

Table 3: Strains used in this study

Strain	Genotype	Figure
DK1295	*whi5Δ::KanMx4*	Figure 1
DK4074	*CLN2-3XHA::hphNT1*	Figure 1
DK4102	*CLN2-3XHA::hphNT1, whi5Δ::KanMX4*	Figure 1
DK4108	*CLN2-3XHA::hphNT1, whi5Δ::KanMX4, cln3-Δ177-6XHA::HIS3*	Figure 1
DK4114	*CLN2-3XHA::hphNT1, whi5Δ::KanMX4, cln3Δ::HIS3*	Figure 1
DK4125	*CLN2-3XHA::hphNT1, whi5Δ::KanMX4, GAL1-CLN3::URA3*	Figure 1
DK4032	*MET25-3XHA-CLN2::NatN2, cln3Δ::HIS3*	Figure 2
DK4034	*MET25-3XHA-CLN2::NatN2, cln3-Δ177-6XHA::HIS3*	Figure 2
DK4026	*MET25-3XHA-CLN2::NatN2*	Figure 2, 3
DK4527	*MET25-3XHA-CLN2::NatN2 GAL1-CLN3::URA3*	Figure 3
DK4545	*MET25-3XHA-CLN2::NatN2 swi6Δ::HIS3*	Figure 3
DK4548	*MET25-3XHA-CLN2::NatN2 swi6Δ::HIS3 GAL1-CLN3::URA3*	Figure 3
DK4144	*MET25-3XHA-CLN2::NatN2, cln1Δ::Hygro*	Figure 4
DK4230	*MET25-3XHA-CLN2::NatN2, cln1Δ::Hygro, GAL1-CLN3::URA3*	Figure 4
KA65	*cln1Δ::TRP*	Figure 4
DK186	*wild type*	Figure 4,6, Figure 5-supplement
DK3348	*MYO1-GFP::TRP, SPC42-GFP::HIS3MX6, GAL1-CLN3-3XHA::URA3*	Figure 5
DK3510	*his3::HIS3+TIR1, leu2::LEU2+TIR1, SPC42-mRuby2::KanMX4*	Figure 5
DK3580	*SPC42-yomRuby2::KanMx4, GAL1::URA3*	Figure 5
DK3524	*his3::HIS3+TIR1, leu2::LEU2+TIR1, cln3-AID::KanMX4, SPC42-GFP::Hygro*	Figure 5, Figure 5-supplement
SH184	*cln3Δ::HIS3MX6*	Figure 5, Figure 5-supplement, Table 2
DK303	*CLB2-3XHA::Trp*	Figure 6
DK4153	*pHG-GST::His*	Figure 6
DK4157	*pt-HGT-CLB2-GST::HIS*	Figure 6
DK4210	*pt-HGT-CLN3-10A-GST::HIS*	Figure 6
DK4403	*pt-HGT-CLN3-10A-GST::HIS GAL1-CLN2-3XHA::URA3*	Figure 6
DK4417	*pt-HGT-GST::HIS GAL1-CLN2-3XHA::URA3*	Figure 6
DK4418	*pt-HGT-CLN3-10A-GST::HIS GAL1-CLN2::URA3*	Figure 6
DK3922	*HOF1-3XHA::Trp*	Figure 7
DK3945	*HOF1-3XHA::Trp, cln3-Δ177-6XHA::HIS3*	Figure 7
DK3960	*HOF1-3XHA::Trp, cln3Δ::His3*	Figure 7
DK3991	*HOF1-3XHA::Trp, Cln3-6XHA::HIS3*	Figure 7
DK4218	*NDD1-6XHA::Hygro*	Figure 8
DK4233	*NDD1-6XHA::Hygro, cln3Δ::HIS3*	Figure 8
DK4235	*NDD1-6XHA::Hygro, cln3-Δ177-6XHA::HIS*	Figure 8
DK3099	*cln3-Δ177-6XHA::KanMx4*	Table 2

Figure 1

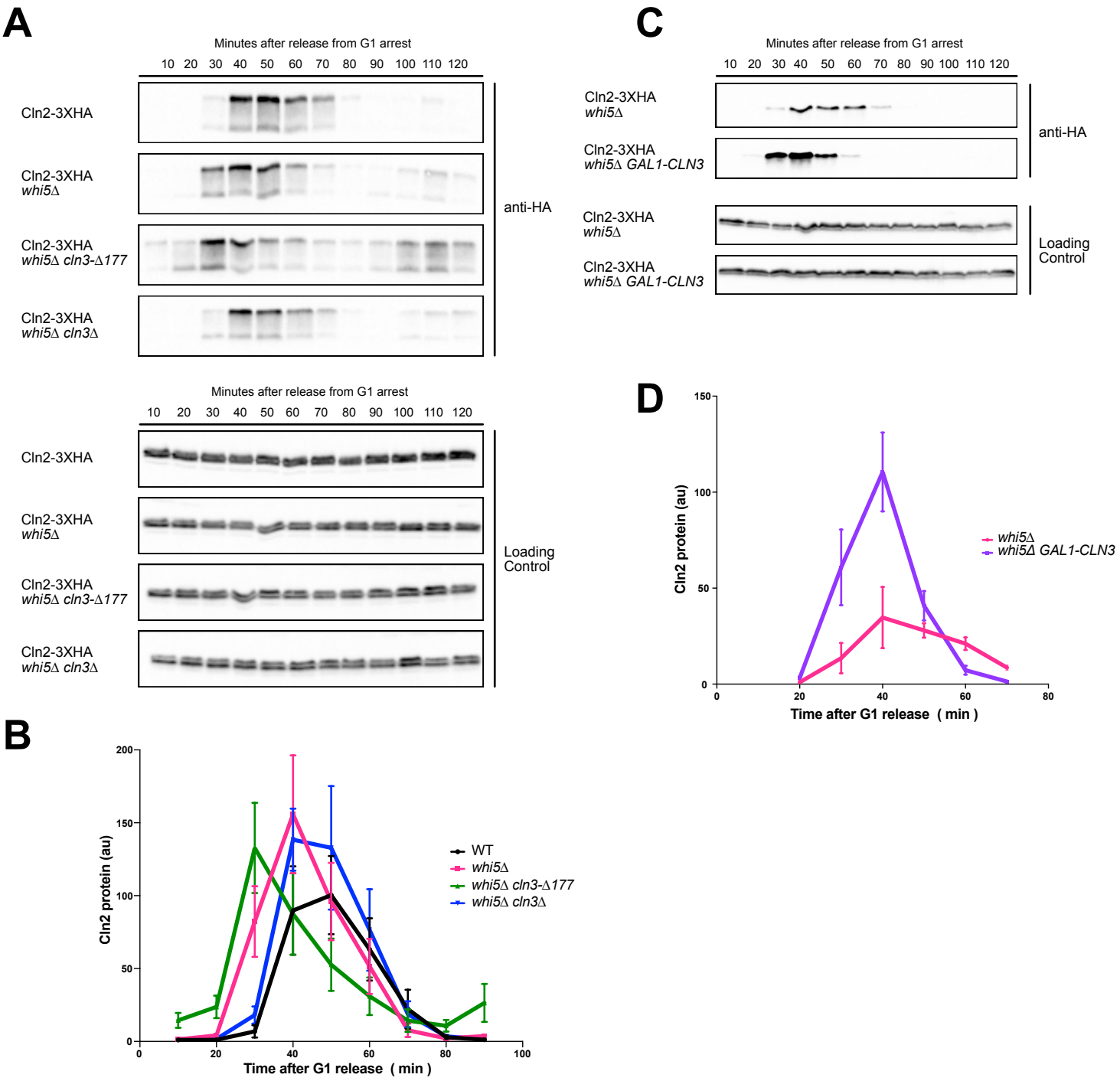
A
Minutes after release from G1 arrest
10 20 30 40 50 60 70 80 90 100 110 120
Cln2-3XHA
Cln2-3XHA whi5Δ
Cln2-3XHA whi5Δ cln3-Δ177
Cln2-3XHA whi5Δ cln3Δ
anti-HA
Minutes after release from G1 arrest
10 20 30 40 50 60 70 80 90 100 110 120
Cln2-3XHA
Cln2-3XHA whi5Δ
Cln2-3XHA whi5Δ cln3-Δ177
Cln2-3XHA whi5Δ cln3Δ
Loading Control
C
Minutes after release from G1 arrest
10 20 30 40 50 60 70 80 90 100 110 120
Cln2-3XHA whi5Δ
Cln2-3XHA whi5Δ GAL1-CLN3
anti-HA
Cln2-3XHA whi5Δ
Cln2-3XHA whi5Δ GAL1-CLN3
Loading Control
D
Cln2 protein (au)
Time after G1 release (min)
whi5Δ
whi5Δ GAL1-CLN3
B
Cln2 protein (au)
Time after G1 release (min)
WT
whi5Δ
whi5Δ cln3-Δ177
whi5Δ cln3Δ

Figure 2

A

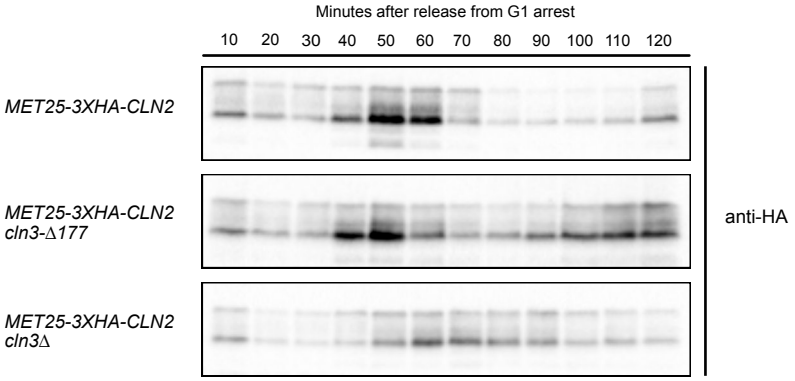
Minutes after release from G1 arrest
10 20 30 40 50 60 70 80 90 100 110 120
MET25-3XHA-CLN2
MET25-3XHA-CLN2 cln3-Δ177
MET25-3XHA-CLN2 cln3Δ
anti-HA

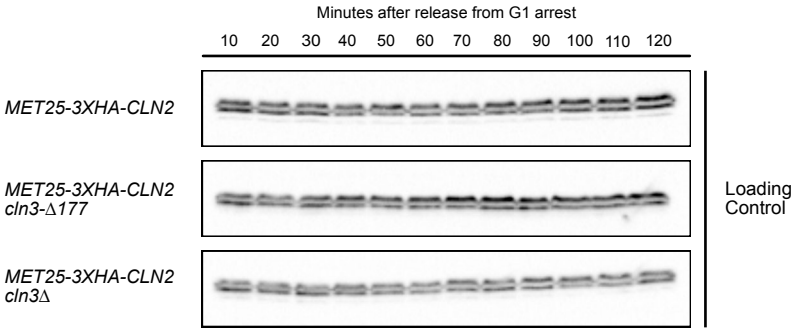
Minutes after release from G1 arrest
10 20 30 40 50 60 70 80 90 100 110 120
MET25-3XHA-CLN2
MET25-3XHA-CLN2 cln3-Δ177
MET25-3XHA-CLN2 cln3Δ
Loading Control

B

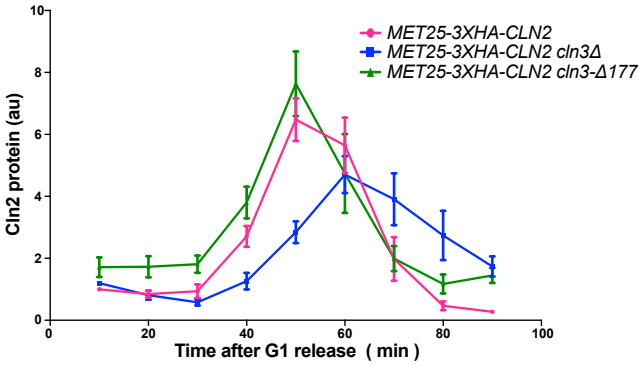
MET25-3XHA-CLN2
MET25-3XHA-CLN2 cln3Δ
MET25-3XHA-CLN2 cln3-Δ177
Cln2 protein (au)
0
2
4
6
8
10
0
20
40
60
80
100
Time after G1 release (min)

Figure 3

A

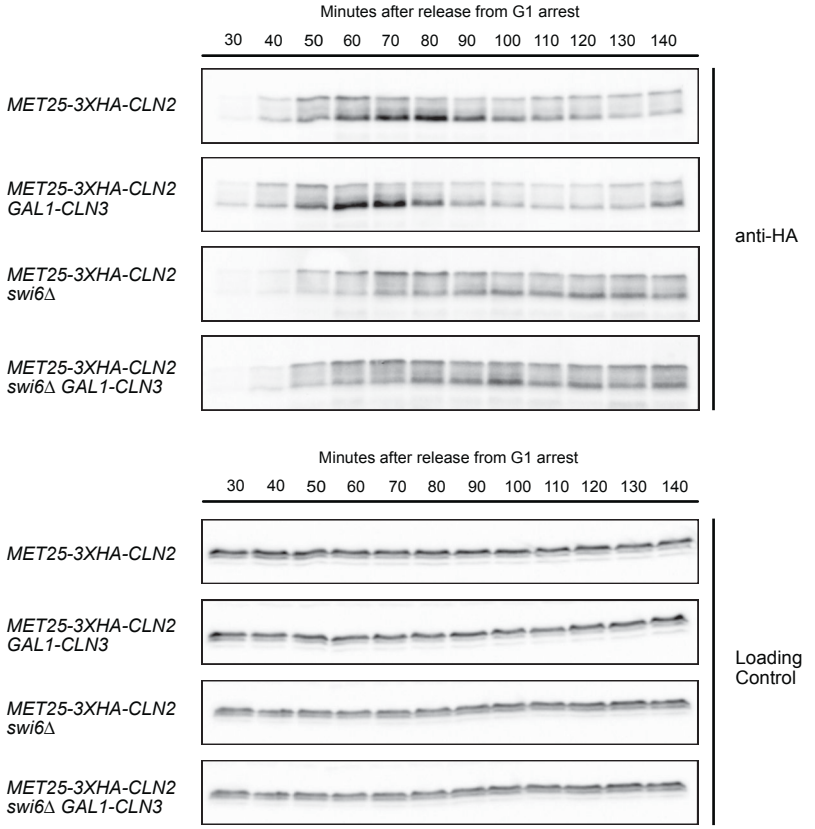
Minutes after release from G1 arrest
30 40 50 60 70 80 90 100 110 120 130 140
MET25-3XHA-CLN2
MET25-3XHA-CLN2 GAL1-CLN3
MET25-3XHA-CLN2 swi6Δ
MET25-3XHA-CLN2 swi6Δ GAL1-CLN3
anti-HA
Minutes after release from G1 arrest
30 40 50 60 70 80 90 100 110 120 130 140
MET25-3XHA-CLN2
MET25-3XHA-CLN2 GAL1-CLN3
MET25-3XHA-CLN2 swi6Δ
MET25-3XHA-CLN2 swi6Δ GAL1-CLN3
Loading Control

B

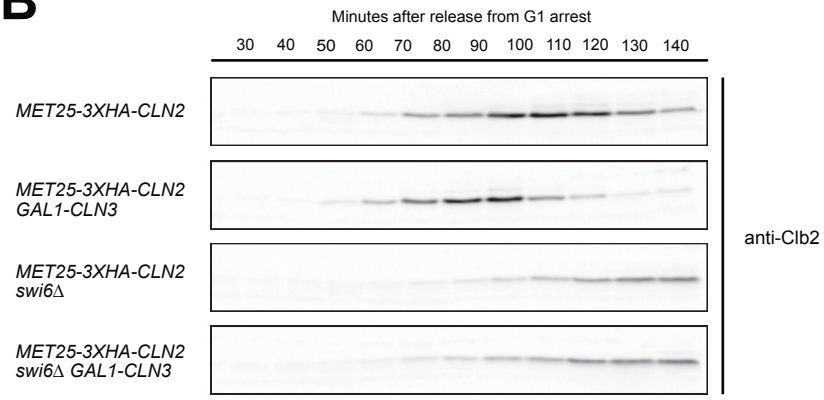
Minutes after release from G1 arrest
30 40 50 60 70 80 90 100 110 120 130 140
MET25-3XHA-CLN2
MET25-3XHA-CLN2 GAL1-CLN3
MET25-3XHA-CLN2 swi6Δ
MET25-3XHA-CLN2 swi6Δ GAL1-CLN3
anti-Clb2

Figure 4

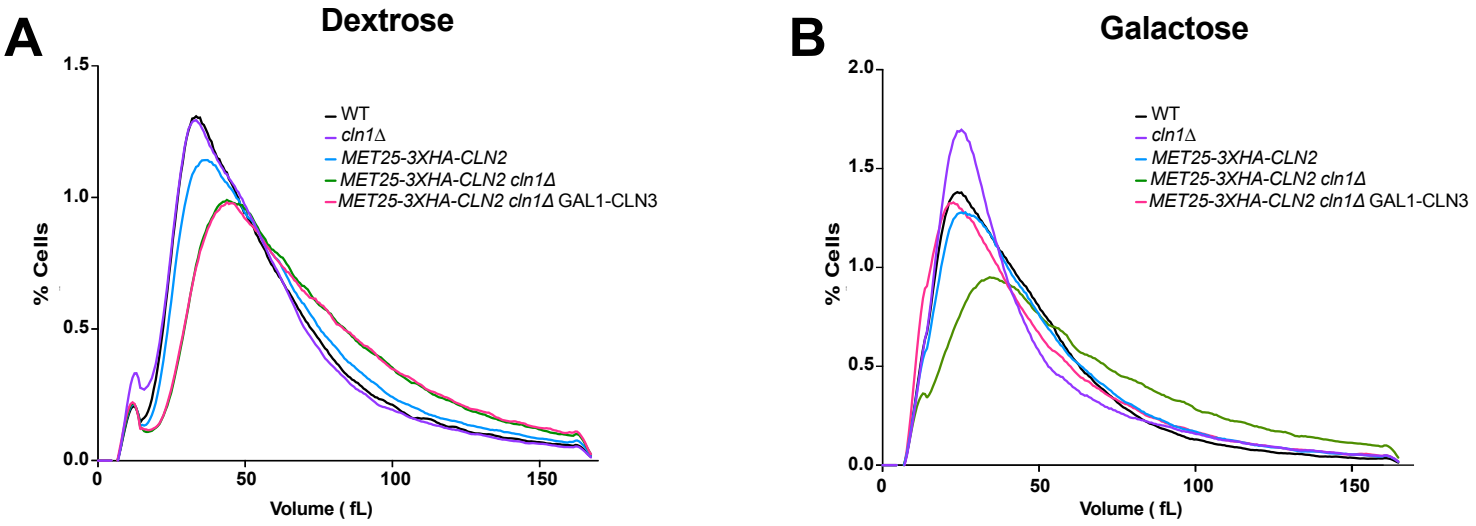
A
Dextrose
% Cells
Volume (fL)
WT
cln1Δ
MET25-3XHA-CLN2
MET25-3XHA-CLN2 cln1Δ
MET25-3XHA-CLN2 cln1Δ GAL1-CLN3
B
Galactose
% Cells
Volume (fL)
WT
cln1Δ
MET25-3XHA-CLN2
MET25-3XHA-CLN2 cln1Δ
MET25-3XHA-CLN2 cln1Δ GAL1-CLN3

Figure 5

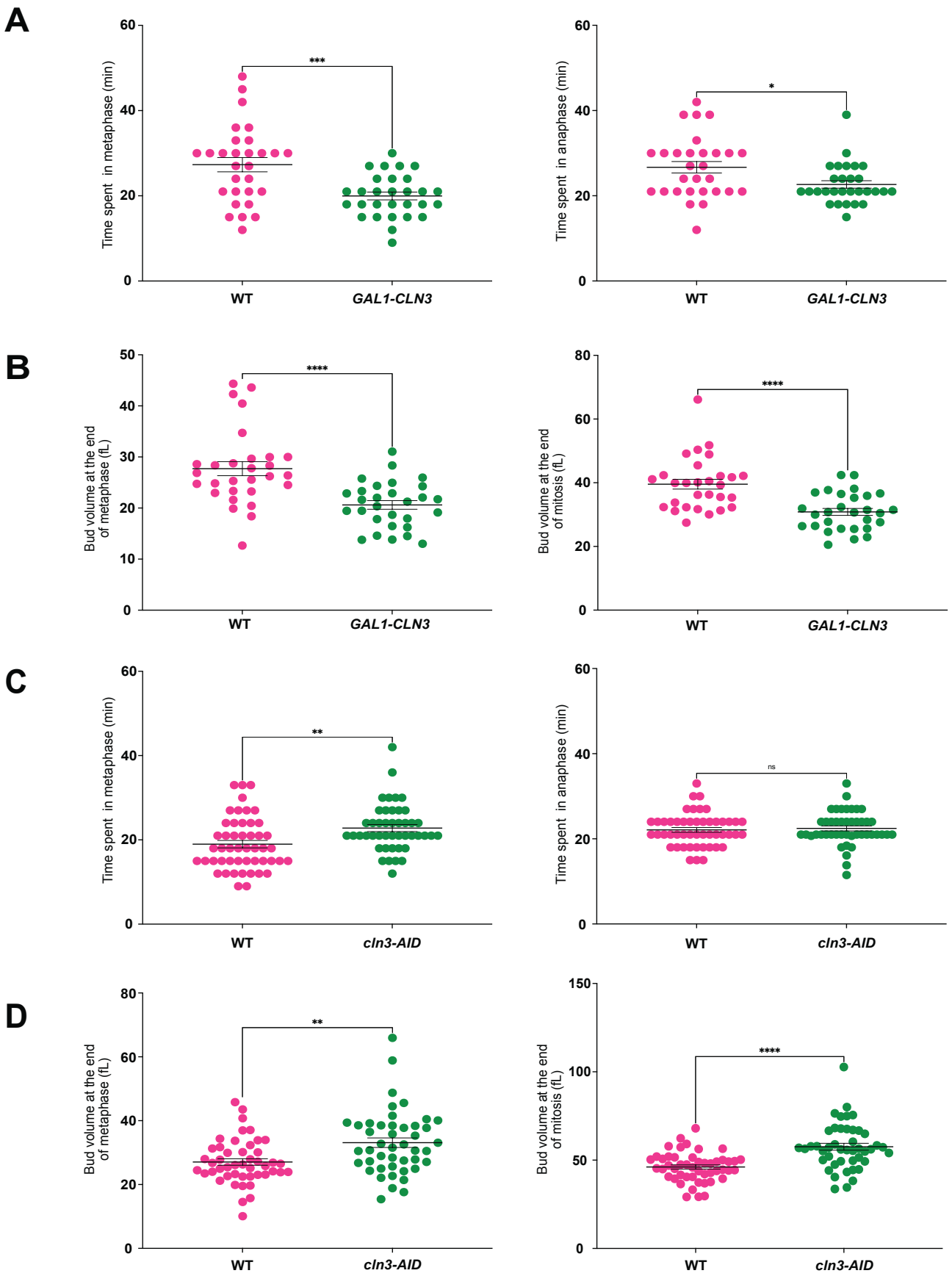
A
Time spent in metaphase (min)
60
40
20
0
***
WT
GAL1-CLN3
Time spent in anaphase (min)
60
40
20
0
*
WT
GAL1-CLN3
B
Bud volume at the end of metaphase (fL)
50
40
30
20
10
0
****
WT
GAL1-CLN3
Bud volume at the end of mitosis (fL)
80
60
40
20
0
****
WT
GAL1-CLN3
C
Time spent in metaphase (min)
60
40
20
0
**
WT
cln3-AID
Time spent in anaphase (min)
60
40
20
0
ns
WT
cln3-AID
D
Bud volume at the end of metaphase (fL)
80
60
40
20
0
**
WT
cln3-AID
Bud volume at the end of mitosis (fL)
150
100
50
0
****
WT
cln3-AID

Figure 5 - figure supplement

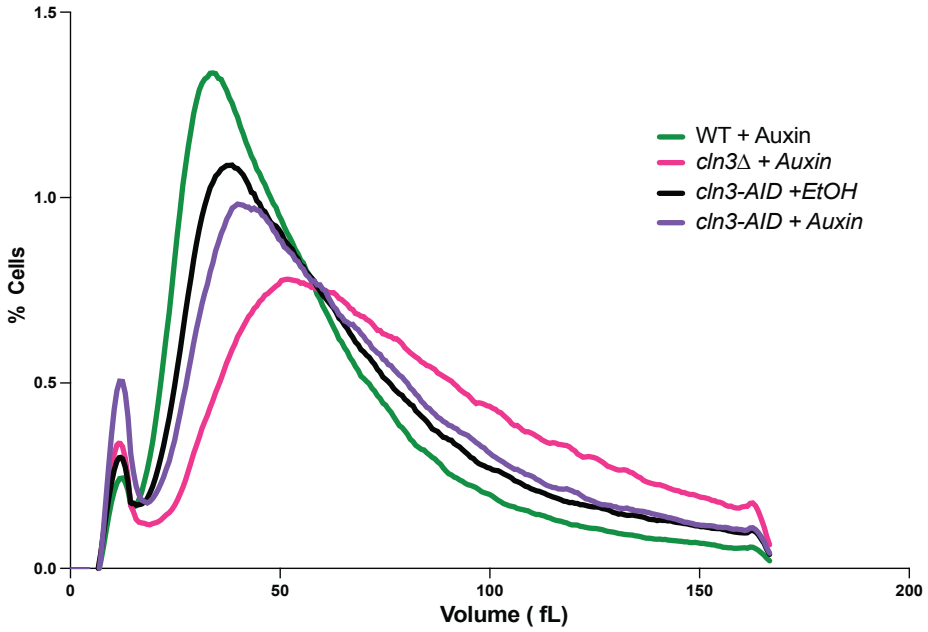

Figure 6

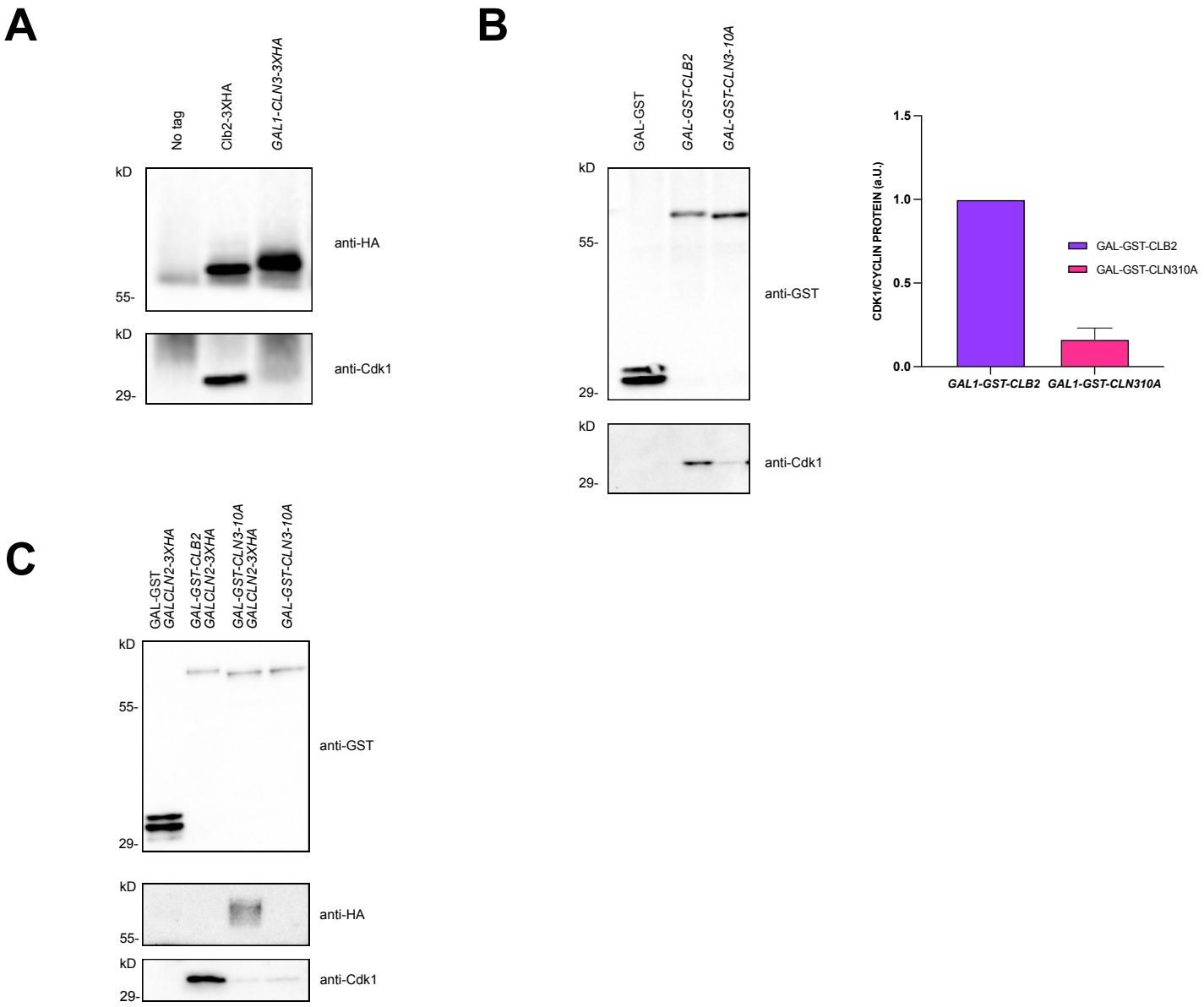
A
No tag
Clb2-3XHA
GAL1-CLN3-3XHA
kD
55-
anti-HA
kD
29-
anti-Cdk1
B
GAL-GST
GAL-GST-CLB2
GAL-GST-CLN3-10A
kD
55-
anti-GST
29-
kD
29-
anti-Cdk1
CDK1/CYCLIN PROTEIN (a.U.)
1.5
1.0
0.5
0.0
GAL-GST-CLB2
GAL-GST-CLN310A
GAL1-GST-CLB2
GAL1-GST-CLN310A
C
GAL-GST GALCLN2-3XHA
GAL-GST-CLB2 GALCLN2-3XHA
GAL-GST-CLN3-10A GALCLN2-3XHA
GAL-GST-CLN3-10A
kD
55-
anti-GST
29-
kD
55-
anti-HA
kD
29-
anti-Cdk1

Figure 7

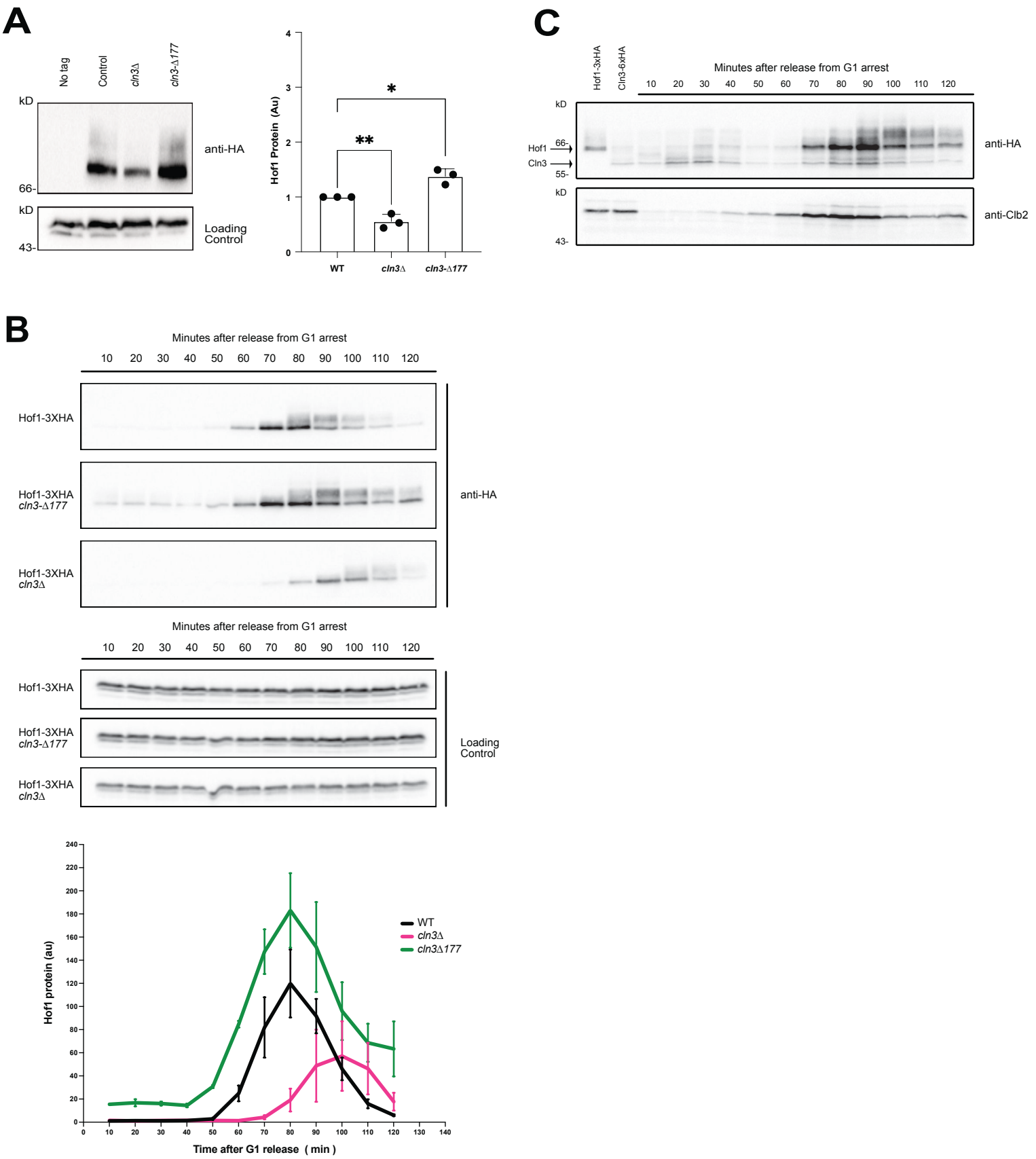
A
No tag
Control
cln3Δ
cln3-Δ177
kD
66-
anti-HA
kD
43-
Loading Control
Hof1 Protein (Au)
WT
cln3Δ
cln3-Δ177
B
Minutes after release from G1 arrest
10 20 30 40 50 60 70 80 90 100 110 120
Hof1-3XHA
Hof1-3XHA cln3-Δ177
Hof1-3XHA cln3Δ
anti-HA
Loading Control
Hof1 protein (au)
Time after G1 release (min)
WT
cln3Δ
cln3Δ177
C
Hof1-3xHA
Cln3-6xHA
Hof1
Cln3
55-
anti-Clb2

Figure 8

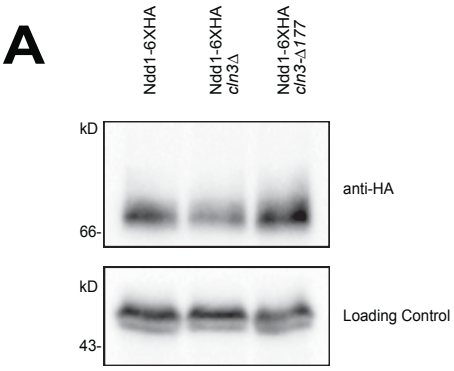
A
Ndd1-6XHA
Ndd1-6XHA cln3Δ
Ndd1-6XHA cln3-Δ177
kD
66-
anti-HA
kD
43-
Loading Control

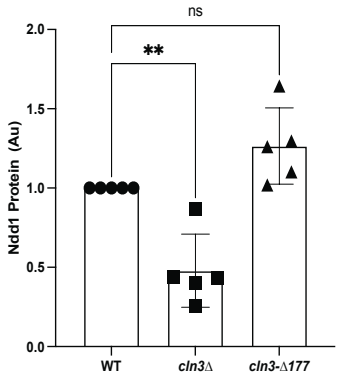
ns
**
2.0
1.5
1.0
0.5
0.0
Ndd1 Protein (Au)
WT
cln3Δ
cln3-Δ177

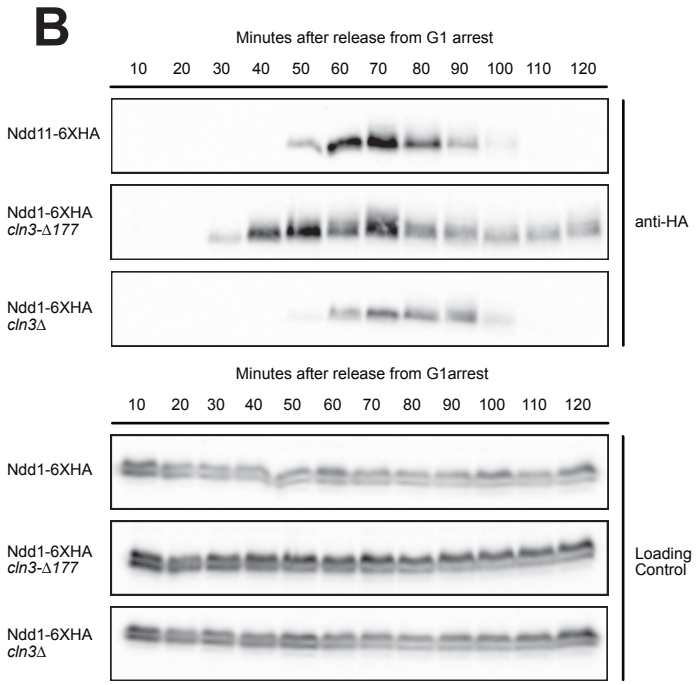
B
Minutes after release from G1 arrest
10 20 30 40 50 60 70 80 90 100 110 120
Ndd11-6XHA
Ndd1-6XHA cln3-Δ177
Ndd1-6XHA cln3Δ
anti-HA
Minutes after release from G1arrest
10 20 30 40 50 60 70 80 90 100 110 120
Ndd1-6XHA
Ndd1-6XHA cln3-Δ177
Ndd1-6XHA cln3Δ
Loading Control

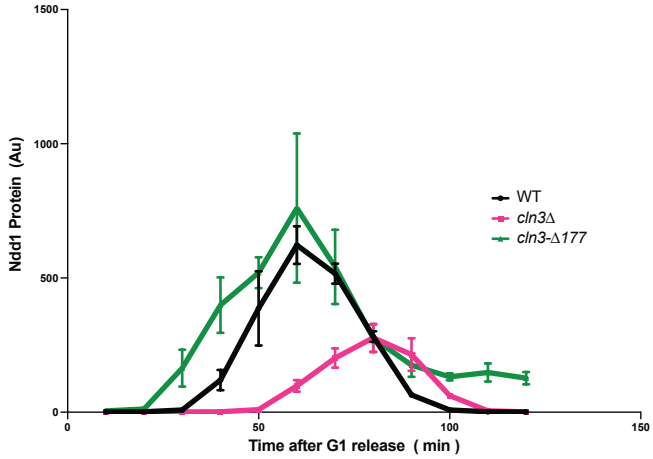
1500
1000
500
0
Ndd1 Protein (Au)
0
50
100
150
Time after G1 release (min)
WT
cln3Δ
cln3-Δ177
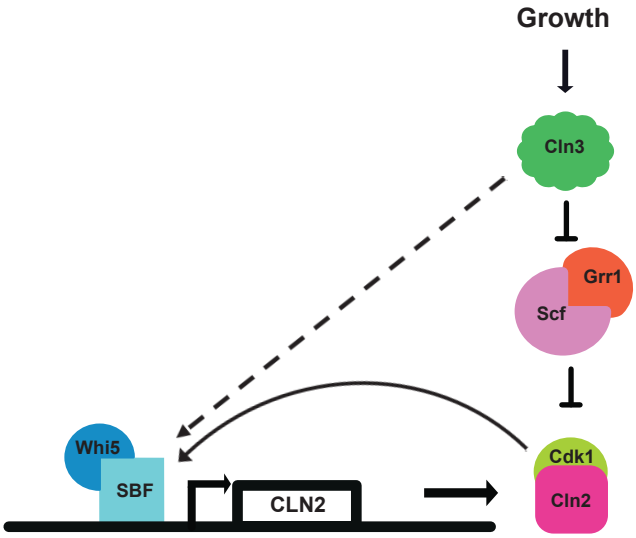
Figure 9